NAM

Computing the Distribution of Pareto Sums using Laplace Transformation and Stehfest Inversion

C. K. Harris and S. J. Bourne

Datum May 2015

Editors Jan van Elk & Dirk Doornhof

General Introduction

In statistical seismology, the properties of distributions of total seismic moment are important for constraining seismological models, such as the strain partitioning model. The total seismic moment is the sum of the moments of individual seismic events, which in common with many other natural processes, are governed by a Pareto or “power law” distributions. In the case of seismicity, the exponent appearing in the power-law relation is small enough for the variance of the distribution to be infinite, which renders standard statistical methods concerning sums of statistical variables, based on the central limit theorem, inapplicable. Determinations of the properties of sums of moderate to large numbers of Pareto distributed variables with infinite variance have traditionally been addressed using intensive Monte-Carlo simulations.

In the calculations for earlier implementations of the strain partitioning model the methods by Zaliapin et al (Ref. 1) was used to determine the properties of such sums. This report presents a novel method for accurate determination of the properties of such sums that is accurate, fast and easily implemented, and is applicable to Pareto-distributed variables for which the power law exponent lies within the interval [0, 1].

This method has been implemented in the seismological models supporting the hazard assessment for induced seismicity in Groningen.

Ref.1 Zaliapin, I.V., Kagan, Y.Y. & Schoenberg, F.P., 2005. Approximating the Distribution of Pareto Sums. *Pure and Applied Geophysics*, 162(6-7), pp.1187–1228. Available at: http://www.springerlink.com/index/10.1007/s00024-004-2666-3 [Accessed November 16, 2012].

NAM

Title	**Computing the Distribution of Pareto Sums using Laplace Transformation and Stehfest Inversion**		**Date**	May 2015
			Initiator	NAM
Author(s)	Chris Harris	**Editors**	Jan van Elk Dirk Doornhof	
Organisation	Shell	**Organisation**	NAM	
Place in the Study and Data Acquisition Plan	Study Theme: Seismological Modelling. Comment: A new mathematical techniques was developed to evaluate Pareto sums.			
Directliy linked research	(1) Seismological Modelling (2) Hazard Assessment			
Used data	None			
Associated organisation	Shell			
Assurance	Internal Assurance only.			

Restricted **SR.15.10646**

Computing the Distribution of Pareto Sums using Laplace Transformation and Stehfest Inversion

by

Christopher K Harris & Stephen J. Bourne (GSNL-PTI/RC)

Shell International Exploration and Production B.V., Rijswijk

Further electronic copies can be obtained from the Global Information Centre.

Executive summary

In statistical seismology, the properties of distributions of total seismic moment are important for constraining seismological models, such as the strain partitioning model [1]. The total seismic moment is the sum of the moments of individual seismic events, which in common with many other natural processes, are governed by a Pareto or "power law" distributions. In the case of seismicity, the exponent β appearing in the power-law relation is small enough for the variance of the distribution to be infinite, which renders standard statistical methods concerning sums of statistical variables, based on the central limit theorem, inapplicable. Determinations of the properties of sums of moderate to large numbers of Pareto distributed variables with infinite variance have traditionally been addressed using intensive Monte-Carlo simulations.

This report presents a novel method for accurate determination of the properties of such sums that is accurate, fast and easily implemented, and is applicable to Pareto-distributed variables for which the power law exponent β lies within the interval [0, 1]. It is based on shifting the original variables so that a non-zero density is obtained exclusively for non-negative values of the parameter and is identically zero elsewhere, a property that is shared by the sum of an arbitrary number of such variables. The technique involves applying the Laplace transform to the normalized sum (which is simply the product of the Laplace transforms of the densities of the individual variables, with a suitable scaling of the Laplace variable), and then inverting it numerically using the Gavers-Stefest algorithm. After validating the method using a number of test cases, it was applied to address the distribution of total seismic moment, and the quantiles computed for various numbers of seismic events were compared with those obtained in the literature using Monte-Carlo simulation. Excellent agreement was obtained.

The speed, accuracy and ease of implementation of the method allows the development of accurate correlations for constraining statistical seismological models using, for example, the maximum likelihood method. It should also be of value in other natural processes governed by Pareto distributions with exponent less than unity.

Table of contents

LIST OF FIGURES

LIST OF FIGURES (CONTINUED)

LIST OF TABLES

1. Introduction

The present work had its origins in the need to estimate total seismic moment released by seismic activity. The probability P($M \rightarrow M + dM$) that the seismic moment associated with an individual event lies in the range M to $M + dM$ varies as

$$P(M \rightarrow M + dM) = f(M)dM \tag{1.1}$$

where the density $f(M)$ takes the form

$$f(M) = \beta M_0^{-1}(M / M_0)^{-(\beta+1)}; M \geq M_0 \tag{1.2}$$

where M_0 is some lower cutoff, for example an observational threshold, and the exponent β lies between 0 and 1, and is believed to be close to 2/3 for many instances of natural and induced seismicity. The distribution $F(M)$ corresponding to $f(M)$ is

$$F(M) = 1 - (M / M_0)^{-\beta}; M \geq M_0 \tag{1.3}$$

The total seismic moment released by a series of N seismic events is then given by

$$M_{TOT} = \sum_{k=1}^{N} M_k \tag{1.4}$$

The most basic model for M_{TOT} assumes that the M_k are independently and identically distributed with the distribution $F(M)$. (Other, more sophisticated models, allow for the presence of aftershocks, but we do not consider this here). Determining the properties of the distribution of M_{TOT} is complicated by the fact that $F(M)$ has infinite variance, so that methods based on the central limit theorem cannot be used. In fact, for $\beta < 1$, the mean of $F(M)$ is also infinite. Zaliapin et al [2] consider various ways of approximating the quantiles of M_{TOT} and validate them with extensive Monte-Carlo simulations. In this report, we work with shifted variables so that the region of non-vanishing density for the resulting variables, and their sums, maps onto the positive real line, permitting use of the Laplace transform. The Laplace transform, which is related to the characteristic function, has the property that the Laplace transform of the sum of variables is simply the product of the Laplace transforms of the individual variables. This is explained in Chapter 2, which also details some properties of the Laplace transform of a Pareto-distributed variable. Chapter 3 describes the Gavers-Stehfest algorithm for numerical inversion of Laplace transforms, which is then applied to three test cases in Chapter 4. Chapter 5 then applies the technique to the same problem as addressed in [2], and compares the results with those presented in [2]. Finally, the report is rounded off with some conclusions and recommendations in Chapter 6.

2. Sums of Shifted Pareto-Distributed Variables and Laplace Transformation

We work with variables normalized with respect to the cut-off M_0 and with sums normalized with respect to a power of N.

$$X_N = N^{-\alpha}\sum_{k=1}^{N} x_k \tag{2.1}$$

where the x_k are IID variables drawn from the Pareto distribution with density

$$f(x) = \beta x^{-(1+\beta)}; x \geq 1$$
$$= 0\,; \text{otherwise} \tag{2.2}$$

We show shortly that a natural choice for the exponent α is

$$\alpha = 1/\beta \tag{2.3}$$

The region over which the density of X_N, which we denote by $f_N(X_N)$ is non-zero varies with N, and corresponds to the portion of the real line greater than or equal to $N^{(1-\alpha)}$. Instead we work with the shifted variables

$$t_k = x_k - 1 \tag{2.4}$$

and their normalized sums

$$T_N = N^{-\alpha}\sum_{k=1}^{N} t_k \tag{2.5}$$

where the t_k are IID variables drawn from the shifted Pareto distribution with density

$$g(t) = \beta(1+t)^{-(1+\beta)}; t \geq 0$$
$$= 0\,; \text{otherwise} \tag{2.6}$$

Clearly,

$$X_N = T_N + N^{(1-\alpha)} \tag{2.7}$$

Denoting the density of T_N by $g_N(T_N)$, we see that, for each value of N, g_N can be non-zero anywhere along the non-negative real line. Taking the Laplace transform of g_N we have

$$\tilde{g}_N(s) = \int_0^\infty dt_1 g(t_1) \int_0^\infty dt_2 g(t_2) \ldots \int_0^\infty dt_N g(t_N) \exp(-sN^{-\alpha}\sum_{k=1}^{N} t_k)$$
$$= < \exp(-sN^{-\alpha}\sum_{k=1}^{N} t_k) > = \tilde{g}^N(s/N^\alpha) \tag{2.8}$$

where

$$\tilde{g}(s) = \beta \int_0^\infty dt(1+t)^{-(1+\beta)} \exp(-st) \tag{2.9}$$

Hence, as stated in the Introduction, the Laplace transform of the normalized sum of shifted Pareto-distributed variables is the product of the Laplace transforms of the individual variables, using a normalized Laplace space variable. This means that, given an efficient algorithm for inverting the Laplace transform, properties of the distribution of the sum of shifted Pareto-distributed variables can be readily computed, and can easily be related back to the distribution of the sum of the original variables using Eq. (2.7). As explained in Chapters 3 and 4, the Gavers-Stehfest algorithm fulfils this requirement. In the following section, we list some properties of $\tilde{g}(s)$, relating it to known special functions and developing direct and asymptotic expansions. We should point out that s is assumed to be real throughout this report.

2.1 Summary of the Properties of the Laplace Transform of a Single Shifted Pareto-Distributed Variable

2.1.1 Expression in Terms of Known Special Functions

Starting from Eq. (2.9), we transform back to the original variable x and write

$$\tilde{g}(s) = \exp(s) \int_1^\infty dx x^{-(1+\beta)} \exp(-sx) \tag{2.10}$$

Rearranging the right-hand side of Eq. (2.10) by integrating by parts, we obtain

$$\tilde{g}(s) = -e^s \left[x^{-\beta} \exp(-sx)\right]_1^\infty - e^s s \int_1^\infty dx x^{-\beta} \exp(-sx)$$

$$= 1 - e^s s \int_1^\infty dx x^{-\beta} \exp(-sx) \tag{2.11}$$

Making the transformation of variable $u = sx$ in Eq. (2.11) we obtain

$$\tilde{g}(s) = 1 - e^s s^\beta \int_s^\infty du u^{-\beta} \exp(-u) \tag{2.12}$$

The right hand side of Eq. (2.12) can nbe expressed in terms of Gamma functions as follows:

$$\tilde{g}(s) = 1 - e^s s^\beta \Gamma(1-\beta) \Gamma_C(1-\beta, s) \tag{2.13}$$

where $\Gamma(a)$ and $\Gamma_C(a, s)$ denote the complete and complementary incomplete Gamma functions respectively, given by

$$\Gamma(a) \equiv \int_0^\infty du u^{a-1} \exp(-u) \tag{2.14}$$

and $\Gamma_C(a,s) \equiv \int_s^\infty du u^{a-1} \exp(-u)/\Gamma(a)$ (2.15)

2.1.2 Series Expansion

Eq. (2.12) may readily be manipulated to obtain a series expansion for $\tilde{g}(s)$ in powers of *s*. We write, making use of the definition in Eq. (2.14),

$$\tilde{g}(s) = 1 - e^s s^\beta \left\{ \Gamma(1-\beta) - \int_0^s du u^{-\beta} \exp(-u) \right\} \tag{2.16}$$

The remaining integral on the right-hand side of Eq. (2.16) may now be expanded out in a series by expanding the exponential and integrating term by term, yielding the result

$$\tilde{g}(s) = 1 - \left\{ \Gamma(1-\beta) s^\beta - \sum_{n=0}^{\infty} \frac{(-1)^n s^{n+1}}{n!(n+1-\beta)} \right\} \exp(s) \tag{2.17}$$

We note that the series converges for all values of *s*, but that using it to evaluate $\tilde{g}(s)$ will be inefficient if *s* is too great, as individual terms of the alternating series will become very large as *n* increases, before dwindling again, resulting in a rounding issue for fixed precision.

2.1.3 Asymptotic Expansion

An asymptotic expansion valid for large *s* may be obtained directly from Eq. (2.9) by making use of the expansion

$$\beta(1+t)^{-1-\beta} = \sum_{n=1}^{\infty} (-1)^{n-1} \frac{\Gamma(n+\beta)}{\Gamma(\beta)} \frac{t^{n-1}}{n!} \tag{2.18}$$

Substituting Eq. (2.18) back into Eq. (2.9) and performing term by term integration yields the following result:

$$\tilde{g}(s) = \sum_{n=1}^{\infty} (-1)^{n-1} \frac{\Gamma(n+\beta)}{\Gamma(\beta) s^n} \tag{2.19}$$

The series on the right-hand side of Eq. (2.19) is to be interpreted in a formal sense only as it diverges for all values of *s*. None-the-less it can give useful estimates of $\tilde{g}(s)$ for *s* large enough by truncating it at the smallest term.

2.2 The Choice of the Parameter α and the Asymptotic Stable Distributions

Returning to Eq. (2.8), we substitute the series expansion given in Eq. (2.17) into the right-hand side to obtain

$$\tilde{g}_N(s) = \left[1 - \left\{\Gamma(1-\beta)\frac{s^\beta}{N^{\alpha\beta}} - \frac{1}{N^\alpha}\sum_{n=0}^{\infty}\frac{(-1)^n s^{n+1}}{n!(n+1-\beta)N^{n\alpha}}\right\}\exp(s/N^\alpha)\right]^N \tag{2.20}$$

Recalling that $\beta < 1$, we see from the form of the right-hand side of Eq. (2.20) that if we choose $\alpha = 1/\beta$, taking the limit $N \to \infty$ results in an expression that is independent of N. Specifically, we have

$$\underset{N\to\infty}{Lt}\ \tilde{g}_N(s) = \tilde{g}_\infty(s) = \exp\{-\gamma s^\beta\} \tag{2.21}$$

where $\gamma = \Gamma(1-\beta)$ (2.22)

The densities $g_\infty(t)$ are known as the asymptotic stable distributions and are a set of distributions to which suitably normalized sums of long-tailed variables with infinite variance converge. In [2], the quantiles of the stable distributions, for which tabulations exist – see e.g. [3] – were considered as estimators of the corresponding quantiles for normalized finite sums of Pareto distributions. This work will be analysed in more detail in Chapter 5. Closed form expressions for $g_\infty(t)$ exist in a few cases, as will be listed in the subsections below, where we restrict ourselves in this report to $\beta < 1$ (asymptotic stable distributions can also be defined for $1 < \beta < 2$, but the analysis is more complicated as the mean is finite and has to be subtracted off separately). Before proceeding to specific cases, we note that the parameter γ just appears as a scale factor in the stable density $g_\infty(t;\gamma)$, where now we have included γ as a label explicitly in the density. Specifically

$$g_\infty(t;\gamma) = \gamma^{-1/\beta} g_\infty(t/\gamma^{1/\beta};1) \tag{2.23}$$

with $g_\infty(t;1) = L^{-1}\left[\tilde{g}_\infty(s;1)\right] = L^{-1}\left[\exp(-s^\beta)\right]$ (2.24)

2.2.1 Asymptotic Stable Distribution for β = ½

This may be obtained by inverting the Laplace transform using the identity

$$\sqrt{\frac{\pi}{a}}\exp(-2\sqrt{ab}) = \int_0^\infty dt\, t^{-1/2}\exp(-at - b/t)\ ;\ a > 0,\ b \geq 0 \tag{2.25}$$

Differentiating Eq. (2.25) with respect to b we have

$$\sqrt{\frac{\pi}{b}}\exp(-2\sqrt{ab}) = \int_0^\infty dt t^{-3/2}\exp(-at - b/t);\ a > 0,\ b > 0 \tag{2.26}$$

Rearranging Eq. (2.26) yields the result

$$\exp(-2\sqrt{ab}) = \sqrt{\frac{b}{\pi}}\int_0^\infty dt t^{-3/2}\exp(-at - b/t) \tag{2.27}$$

Setting $a = s$ and $b = \gamma^2/4$ means that the left-hand side of Eq. (2.27) may be identified as $\tilde{g}_\infty(s)$ and we deduce that

$$g_\infty(t) = \frac{\gamma}{2\sqrt{\pi}}t^{-3/2}\exp\{-\gamma^2/(4t)\} \tag{2.28}$$

2.2.2 Asymptotic Stable Distribution for β = ¼

In this case we may use Eq. (2.26) again, replacing t by u, setting $b = \gamma^2/4$ as before, and this time setting $a = s^{1/2}$. Then

$$\exp(-\gamma s^{1/4}) = \frac{\gamma}{2\sqrt{\pi}}\int_0^\infty du u^{-3/2}\exp\{-s^{1/2}u - \gamma^2/(4u)\} \tag{2.29}$$

Since $L^{-1}[\exp(-s^{1/2}u)] = \frac{u}{2\sqrt{\pi}}t^{-3/2}\exp\{-u^2/(4t)\}$ (2.30)

we deduce that

$$g_\infty(t) = L^{-1}\left[\exp(-\gamma s^{1/4})\right] = \frac{\gamma}{4\pi}t^{-3/2}\int_0^\infty du u^{-1/2}\exp\{-u^2/(4t) - \gamma^2/(4u)\} \tag{2.31}$$

Let $u = t^{1/3}\gamma^{2/3}v$ (2.32)

Then $g_\infty(t) = \frac{\gamma^{4/3}}{4\pi}t^{-4/3}\int_0^\infty dv v^{-1/2}\exp\{-\frac{1}{4}\gamma^{4/3}t^{-1/3}(v^2 + 1/v)\}$ (2.33)

2.2.3 Asymptotic Stable Distribution for β = 2/3

In [2], an expression for $g_\infty(t)$ is given in Eq. 15 of that work for $\beta = 2/3$ which is attributed to [4]. It gives an expression for $g_\infty(t; 2)$ in terms of a special function, which, in the present notation, can be written as

$$g_\infty(t;2) = \frac{\sqrt{3}}{\sqrt{\pi}t}\exp\{-16/(27t^2)\}W_{1/2,1/6}\{32/(27t^2)\} \tag{2.31}$$

$W_{\kappa,\mu}(z)$ is a Whittaker function of the second kind [5] and has the integral representation [5]

$$W_{\kappa,\mu}(z) = e^{-z/2} z^{1/2+\mu} \int_0^\infty du e^{-zu} u^{\mu-\kappa-1/2} (1+u)^{\mu+\kappa-1/2} / \Gamma(\tfrac{1}{2}+\mu-\kappa) \tag{2.32}$$

For the specific values of κ and μ appearing in Eq. (2.31), we have

$$W_{1/2,1/6}(z) = e^{-z/2} z^{2/3} \int_0^\infty du e^{-zu} u^{-5/6} (1+u)^{1/6} / \Gamma(\tfrac{1}{6}) \tag{2.33}$$

Substituting Eq. (2.33) back into Eq. (2.31) then yields

$$g_\infty(t;2) = \frac{9}{4\sqrt{2\pi}} e^{-z} z^{7/6} \int_0^\infty du e^{-zu} u^{-5/6} (1+u)^{1/6} / \Gamma(\tfrac{1}{6}) \tag{2.34}$$

with $z = 32/(27t^2)$ (2.35)

Note that, as a check on Eq. (2.35), we have

$$\int_0^\infty dt g_\infty(t;2) = \frac{\sqrt{3}}{2\sqrt{\pi}} \int_0^\infty dz z^{-1/3} \int_0^\infty du e^{-(1+u)z} u^{-5/6} (1+u)^{1/6} / \Gamma(\tfrac{1}{6}) \tag{2.36}$$

Interchanging the order of integration on the right-hand side of Eq. (2.36), and performing the integration over z, we obtain

$$\int_0^\infty dt g_\infty(t;2) = \frac{\sqrt{3}\Gamma(\frac{2}{3})}{2\sqrt{\pi}\Gamma(\frac{1}{6})} \int_0^\infty du u^{-5/6} (1+u)^{-1/2} \tag{2.37}$$

Since (see e.g. [7]),

$$\int_0^\infty du u^{-5/6} (1+u)^{-1/2} = \frac{\Gamma(\frac{1}{6})\Gamma(\frac{1}{3})}{\Gamma(\frac{1}{2})} = \frac{\Gamma(\frac{1}{6})\Gamma(\frac{1}{3})}{\sqrt{\pi}} \tag{2.38}$$

we may write

$$\int_0^\infty dt g_\infty(t;2) = \frac{\sqrt{3}}{2\pi} \Gamma(\tfrac{2}{3})\Gamma(\tfrac{1}{3}) \tag{2.39}$$

According to the reflection theorem for the Gamma function [8],

$$\Gamma(\nu)\Gamma(1-\nu) = \pi / \sin(\pi\nu) \tag{2.40}$$

In the present case, we have

$$\Gamma(1/3)\Gamma(2/3) = \pi / \sin(\pi/3) = \pi /(\sqrt{3}/2) \tag{2.41}$$

Hence we establish the expected result that

$$\int_0^\infty dtg_\infty(t;2) = 1 \tag{2.42}$$

3. The Stehfest Algorithm for Numerical Laplace Transform Inversion

The Gaver-Stehfest algorithm [9, 10] used in this report can be seen as a member of a class of algorithms in which, at any given time, the solution in real time is represented as a weighted finite linear combination of transform values at n specific nodes [11]. The n weights and nodes, w_1, w_2 ... w_n and α_1, α_2 ... α_n respectively are in general complex numbers depending on n, but not necessarily on the specific form of the transform or the time t. More specifically, we write

$$f(t) = \sum_{k=1}^{n} (w_k / t)\tilde{f}(\alpha_k / t) \tag{3.1}$$

The form of (3.1) can be motivated by considering the exact expression for the inverse Laplace transform which is given by

$$f(t) = \underset{R_C \to \infty}{Lt} \frac{1}{2\pi i} \int_{c-iR_C}^{c+iR_C} ds \exp(st)\tilde{f}(s) \tag{3.2}$$

The constant c is chosen to lie to the right of all singularities of $\tilde{f}(s)$ and the integration contour is depicted in Figure 3.1. Making the change of variable

$$s = z/t \tag{3.3}$$

in Figure 3.1, and taking the limit $R_C \to \infty$, we obtain

$$f(t) = \frac{1}{2\pi i t} \int_{c-i\infty}^{c+i\infty} dz \exp(z)\tilde{f}(z/t) \tag{3.4}$$

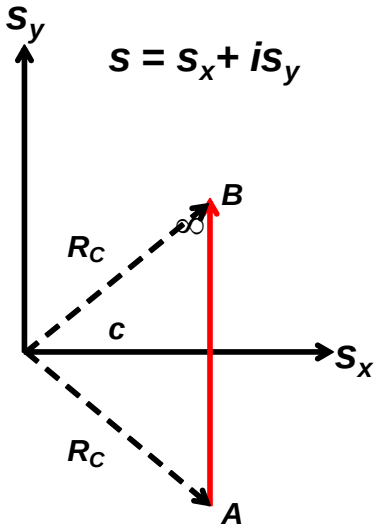

Figure 3.1. Contour AB of Eq. (3.2), Shown in the Complex Plane

We now readily see how a numerical approximation of the integral on the right-hand side of Eq. (3.4) could resemble the right-hand side of Eq. (3.1).

The Gaver-Stehfest algorithm uses the following choice for the weights w_k and nodes α_k

$$w_k = \ln(2)\frac{(-1)^{k+m}}{m!}\sum_{j=[(k+1)/2]}^{\min(k,m)}\binom{m}{j}\binom{2j}{j}\binom{j}{k-j}; k = 1,2...n \; ; \; n = 2m; \; m \geq 1 \tag{3.5}$$

and $$\alpha_k = k\ln(2) \tag{3.6}$$

Note that, in writing Eq. (3.5), n is even and is equal to $2m$. One of the present authors became aware of the Gaver-Stehfest algorithm recently, while working on issues around extra-heavy oil mobilization by in-situ heating [12]. In fact, the reservoir engineering community started to use it shortly after the publication of Stehfest's paper [10] in 1970 [13]. For many problems involving conductive thermal transport in systems with cylindrical symmetry, the form of temperature distributions in Laplace space is much simpler than the form of the corresponding distributions in real time, even when closed-form analytical solutions to the latter are known.

The same conclusion is reached for analogous physical problems such as fluid transport in porous media. Accordingly, numerical inversion of the Laplace transformed solution for temperature, heat flux, pressure and fluid flux for this class of physical problems is often seen as preferable to numerical solution of real-time expressions for these quantities. In the problem treated in [12], which is a generalization of the classic problem of heating a formation using a heat source placed in a borehole, results obtained using Stehfest's algorithm were shown to be extremely accurate. It will be showned in the next chapter that this accuracy is maintained for the class of problems treated in this report.

The coefficients w_k and α_k do not depend on the specific problem to be solved, or the value of t, and have been pre-computed for a large number of values of n. This fact makes the algorithm easy to implement numerically, including in a Microsoft Excel spreadsheet, which is what was done for many of the computations reported here. The expression for α_k given in Eq. (3.6) is straightforward, and we rewrite Eq. (3.1) as

$$f(t) = (\ln(2)/t)\sum_{k=1}^{n}\tilde{w}_k \, \tilde{f}\{\ln(2)k/t\} \tag{3.7}$$

where $$\tilde{w}_k = \frac{(-1)^{k+m}}{m!}\sum_{j=[(k+1)/2]}^{\min(k,m)}\binom{m}{j}\binom{2j}{j}\binom{j}{k-j}; k = 1,2...n; \; n = 2m; \; m \geq 1 \tag{3.8}$$

It is readily observed that the $\tilde{w}_k$ are ratios of integers, and we write

$$\tilde{w}_k = M_k / N_k \tag{3.9}$$

where M_k and N_k are integers such that all common factors have been divided out. Tabulation of M_k, N_k and $\tilde{w}_k$ are shown in Table 3.I(a) for n = 8 & 10, and Table 3.I(b) for n = 12 & 14, which are the four values of n used in the remainder of this report.

Table 3.I (a). Stehfest Algorithm Weights for n =8 and 10

$n = 8$				$n = 10$			
k	M_k	N_k	$\tilde{w}_k$	k	M_k	N_k	$\tilde{w}_k$
1	-1	3	-0.3333	1	1	12	0.0833
2	145	3	48.3333	2	-385	12	-32.0833
3	-906	1	-906.0000	3	1279	1	1279.0000
4	16394	3	5464.6667	4	-46871	3	-15623.6667
5	-43130	3	-14376.6667	5	505465	6	84244.1667
6	18730	1	18730.0000	6	-473915	2	-236957.5000
7	-35840	3	-11946.6667	7	1127735	3	375911.6667
8	8960	3	2986.6667	8	-1020215	3	-340071.6667
				9	328125	2	164062.5000
				10	-65625	2	-32812.5000

Inspecting Tables 3.I, we see that the weights $\tilde{w}_k$ are alternating and increase in absolute magnitude as n increases. Thus increasing the number of nodes will increase the accuracy of the Stehfest algorithm up to the point, assuming fixed precision, at which the computation becomes overwhelmed by the accumulation of rounding errors and the algorithm begins to diverge. This convergence and then divergence can be detected by performing computations for a variety of values of n. Rounding considerations also require the numerical computation of the Laplace transform at the node points $\ln(2)k/t$ to be as accurate as possible.

Table 3.I (b). Stehfest Algorithm Weights for n =12 and 14

$n = 12$				$n = 14$			
k	M_k	N_k	$\tilde{w}_k$	k	M_k	N_k	$\tilde{w}_k$
1	-1	60	-0.0167	1	1	360	0.0028
2	961	60	16.0167	2	-461	72	-6.4028
3	-1247	1	-1247.0000	3	18481	20	924.0500
4	82663	3	27554.3333	4	-6227627	180	-34597.9278
5	-7898425	30	-263280.8333	5	4862890	9	540321.1111
6	13241387	10	1324138.7000	6	-131950391	30	-4398346.3667
7	-116751166	30	-3891705.5333	7	189788326	9	21087591.7778
8	21159859	3	7053286.3333	8	-5755042174	90	-63944913.0444
9	-16010673	2	-8005336.5000	9	2551951591	20	127597579.5500
10	11105661	2	5552830.5000	10	-2041646257	12	-170137188.0833
11	-10777536	5	-2155507.2000	11	4509824011	30	150327467.0333
12	1796256	5	359251.2000	12	-169184323	2	-84592161.5000
				13	824366543	30	27478884.7667
				14	-117766649	30	-3925554.9667

4. Application to Three Test Cases

These three test cases are chosen both to be relevant to the problem that this report is concerned with, and also so that properties of the distributions can be independently determined in order to benchmark the Stehfest algorithm.

4.1 Application to a Single Variable with a Shifted Pareto Distribution

The first test case is the single variable with a shifted Pareto distribution, whose density is given in Eq. (2.6). The corresponding cumulative distribution function $G(t)$ is given by

$$\begin{aligned} G(t) &= 1-(1+t)^{-\beta}; t \geq 0 \\ &= 0 \text{ ; otherwise} \end{aligned} \tag{4.1}$$

Following the framework outlined in the previous chapter, we compute $g(t)$ using the Stehfest algorithm, specifically using (*cf* Eq. 3.7)

$$g(t) = (\ln(2)/t)\sum_{k=1}^{n} \tilde{w}_k \tilde{g}\{\ln(2)k/t\} \tag{4.2}$$

where $\tilde{g}(s)$ is computed using the expressions derived in Section 2.1, specifically Eqs. (2.13), (2.17) and (2.19). Since

$$\tilde{G}(s) = s^{-1}\tilde{g}(s) \tag{4.3}$$

The corresponding expression to (4.2) for $G(t)$ is

$$G(t) = \sum_{k=1}^{n} (\tilde{w}_k / k)\tilde{g}\{\ln(2)k/t\} \tag{4.4}$$

After performing the computations, the results of applying Eqs. (4.2) and (4.4) are compared with the exact results in Eqs. (2.6) and (4.1). A comparison of the results for $\beta = 2/3$ and using eight nodes is shown in Figure 4.1 (a), with the Stehfest algorithm being implemented at values of the shifted Pareto variable of t = 0.1, 0.2, 0.5, 1, 2, 5 & 10. The accuracy of the Stehfest algorithm, in terms of absolute relative error, is less than 0.2% for the density and less than 0.05% for the cumulative distribution function. Individual values for the relative error are shown in Figure 4.1 (b)

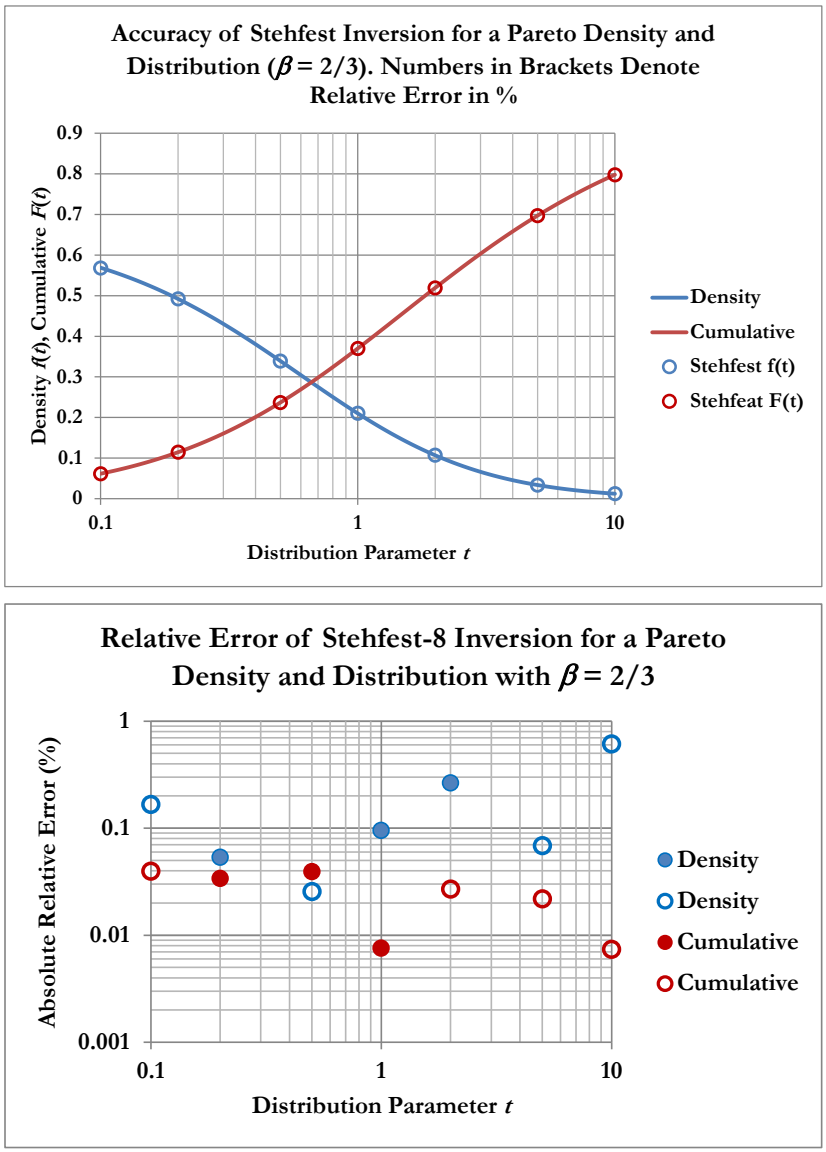

Figure 4.1. (a) Comparison of Stehfest Algorithm Computations with Exact Results for Shifted Pareto Densities and Distributions with $\beta = 2/3$. (b) Relative Error of the Stehfest-8 Inversion, Filled and Open Symbols Denote the Sign of the Relative Error (+ve or –ve Respectively).

4.2 Application to the Asymptotic Stable Densities

4.2.1 Comparison with the FRACDEN Tabulation

The FRACDEN database [3] contains a tabulation of the quantiles of the asymptotic stable densities $g_\infty(t; \gamma)$ for values of β from 0.5 up to unity (and also beyond, up to $\beta = 2$), in steps of 0.02. The quantiles tabulated are 0.0001, 0.001, 0.005, 0.01, then in steps of 0.01 up to 0.99, and subsequently 0.995, 0.999 and 0.9999. They give the value of the parameter t at each quantile, as well as the density. The tabulations are for the specific value $\gamma = \sec(\pi\beta/2)$, but can be scaled for any value of γ using Eq. (2.23). The Stehfest computation was performed for $\gamma = 1$, so that

$$g_{\infty}(t;1) = (\ln(2)/t)\sum_{k=1}^{n} \tilde{w}_k \exp\{-(\ln(2)k/t)^{\beta}\} \tag{4.5}$$

and $$G_{\infty}(t;1) = \sum_{k=1}^{n} (\tilde{w}_k / k)\exp\{-(\ln(2)k/t)^{\beta}\} \tag{4.6}$$

The Stehfest algorithm was performed for β values of 0.5, 0.56, 0.62, 0.68, 0.74 and 0.8 and at quantiles of 10% (0.1), 35% (0.35), 50% (0.5, the median), 65% (0.65), 90% (0.9), 95% (0.95) and 98% (0.98). 14 nodes were used, and Eq. (4.6) was used to tune the value of the parameter t to each quantile and then the density computed using Eq. (4.5). The computed values of t corresponding to each quantile are shown in Figure 4.2, while the relative errors of the Stehfest inversion are plotted in Figure 4.3.

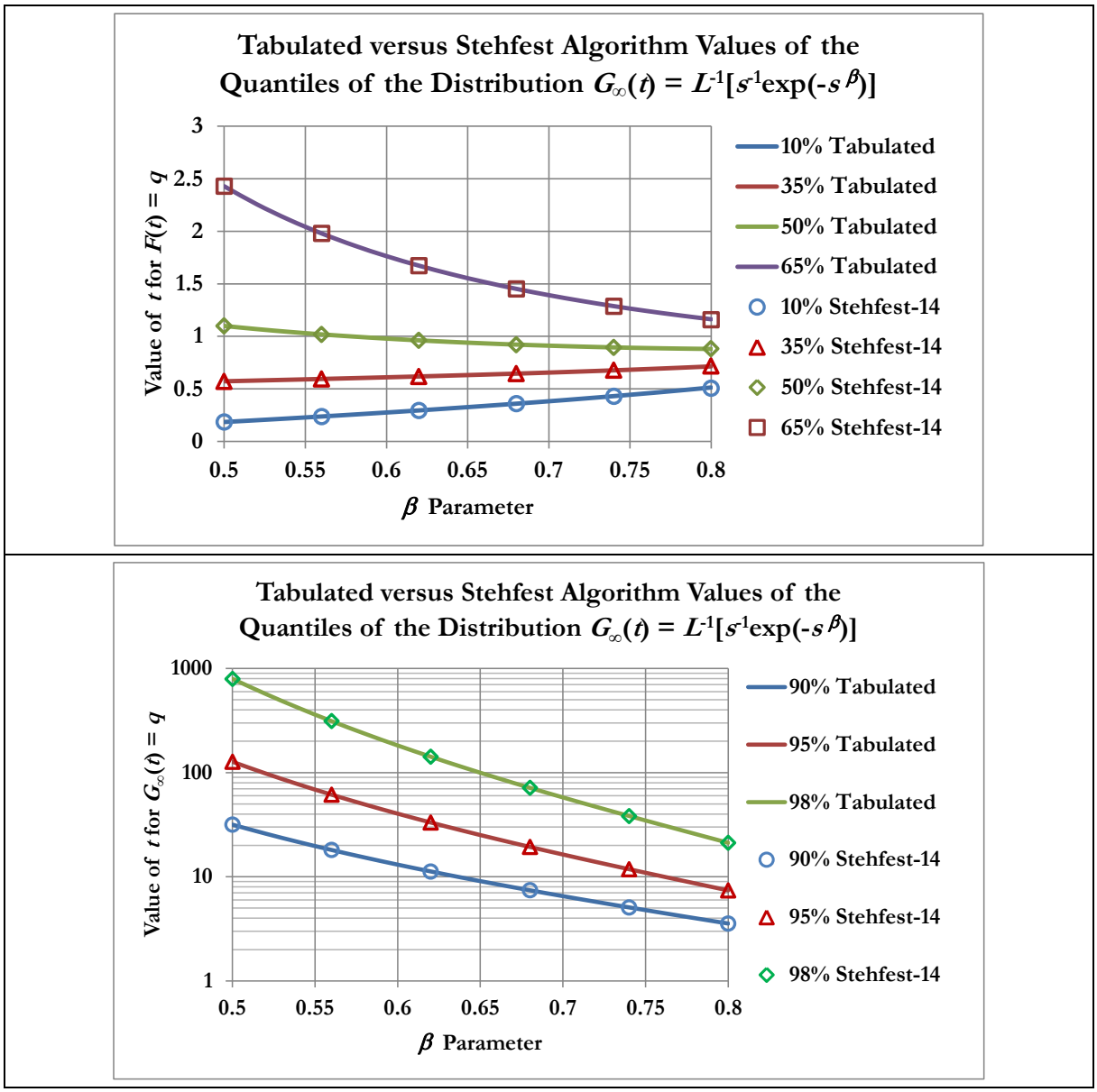

Figure 4.2. Comparison of Stehfest Algorithm Values of the Parameter t Corresponding to Various Quantiles of the Asymptotic Stable Distribution G∞(t) with the FRACDEN [3] Tabulation. (a) 10%, 35%, 50% & 65% Quantiles, (b) 90%, 95% and 98% Quantiles.

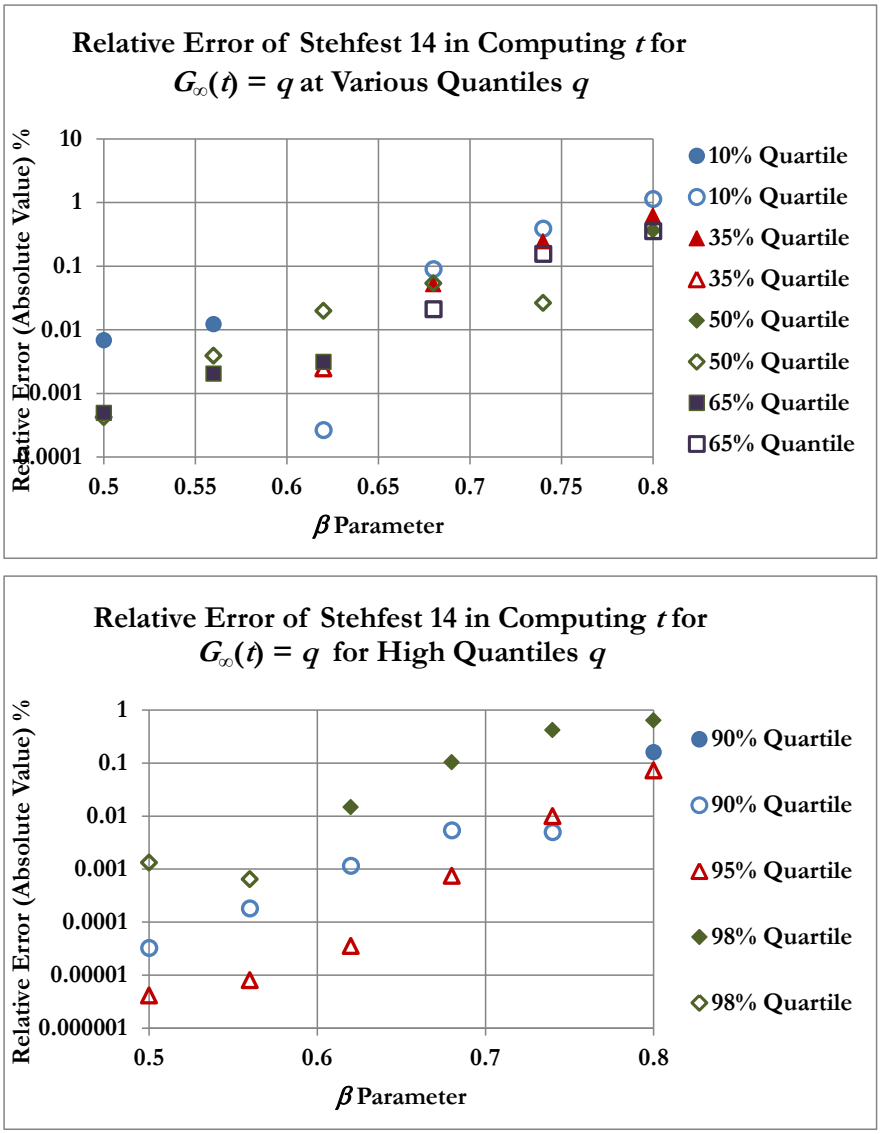

Figure 4.3. Relative Error of Stehfest Algorithm Values of the Parameter t Corresponding to Various Quantiles of the Asymptotic Stable Distribution $G_\infty(t)$ with the FRACDEN [3] Tabulation. (a) 10%, 35%, 50% & 65% Quantiles, (b) 90%, 95% and 98% Quantiles. Symbols are Filled or Open According to Whether the Relative Error is Positive of Negative Respectively.

.

Similarly, the accuracy of the Stehfest computation for the value of the density $g_\infty(t)$ at the above quantiles is shown in Figure 4.4, split up in the same way: Figure 4.4 (a) shows the 10%, 35%, 50% & 65% quantiles while Figure 4.4 (b) shows the 90%, 95% and 98% quantiles. Figure 4.5 displays the corresponding relative errors for the Stehfest computation. Inspection of Figure 4.5 reveals that the accuracy of the Stehfest algorithm for computation of the stable distribution densities is generally greatest for low values of β and falls to give errors of several percent as β approaches 0.8. This is because the density becomes increasingly strongly peaked as β increases. This is seen in Figure 4.6 which shows plots of the asymptotic stable density for $\beta = 0.5$, 0.66 and 0.8.

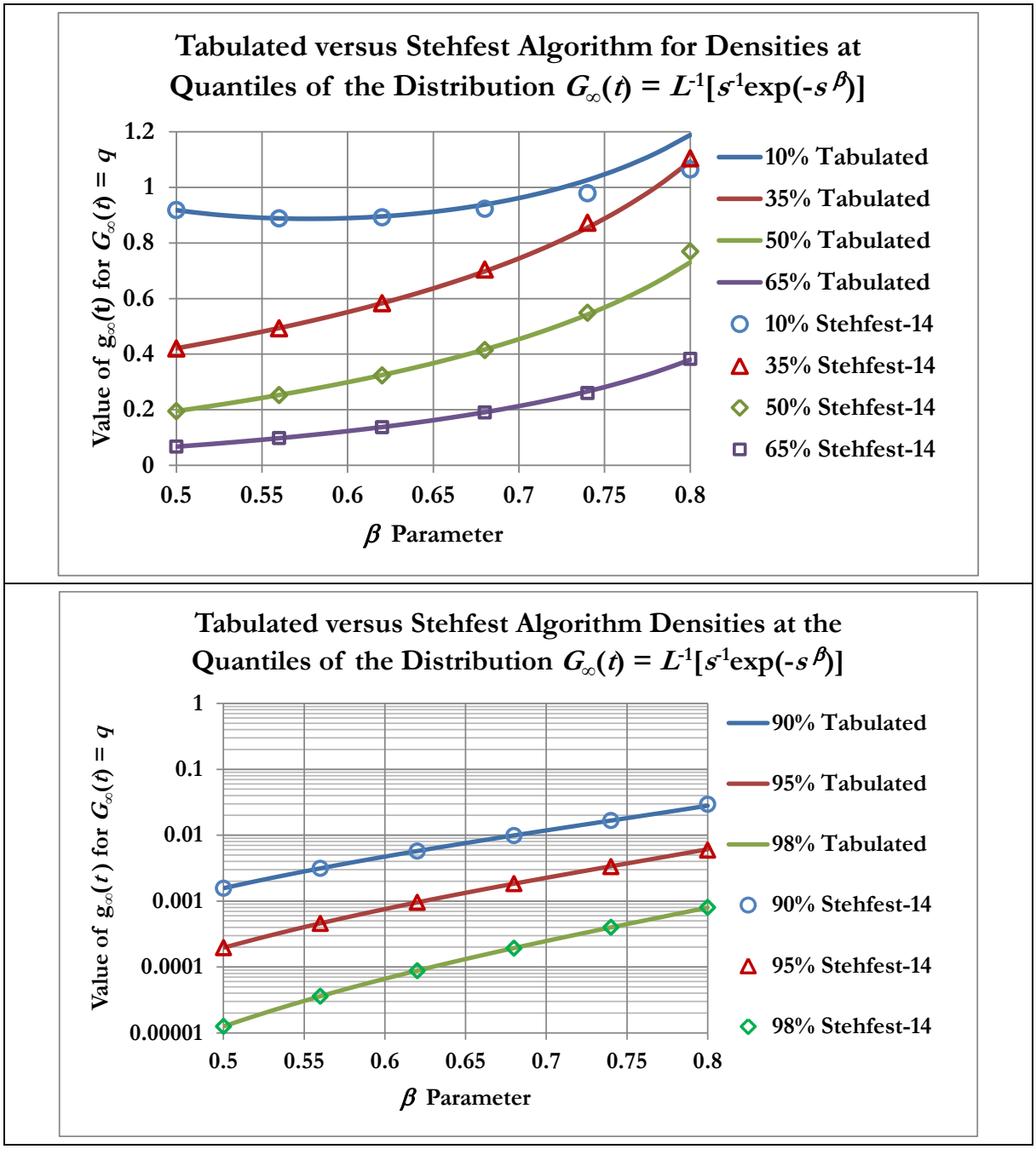

Figure 4.4. Comparison of the the Density $g_\infty(t)$ Computed using the Stehfest Algorithm at Various Quantiles of the Asymptotic Stable Distribution $G_\infty(t)$ with the FRACDEN Tabulations [3] (a) 10%, 35%, 50% & 65% Quantiles. (b) 90%, 95% & 98% Quantiles.

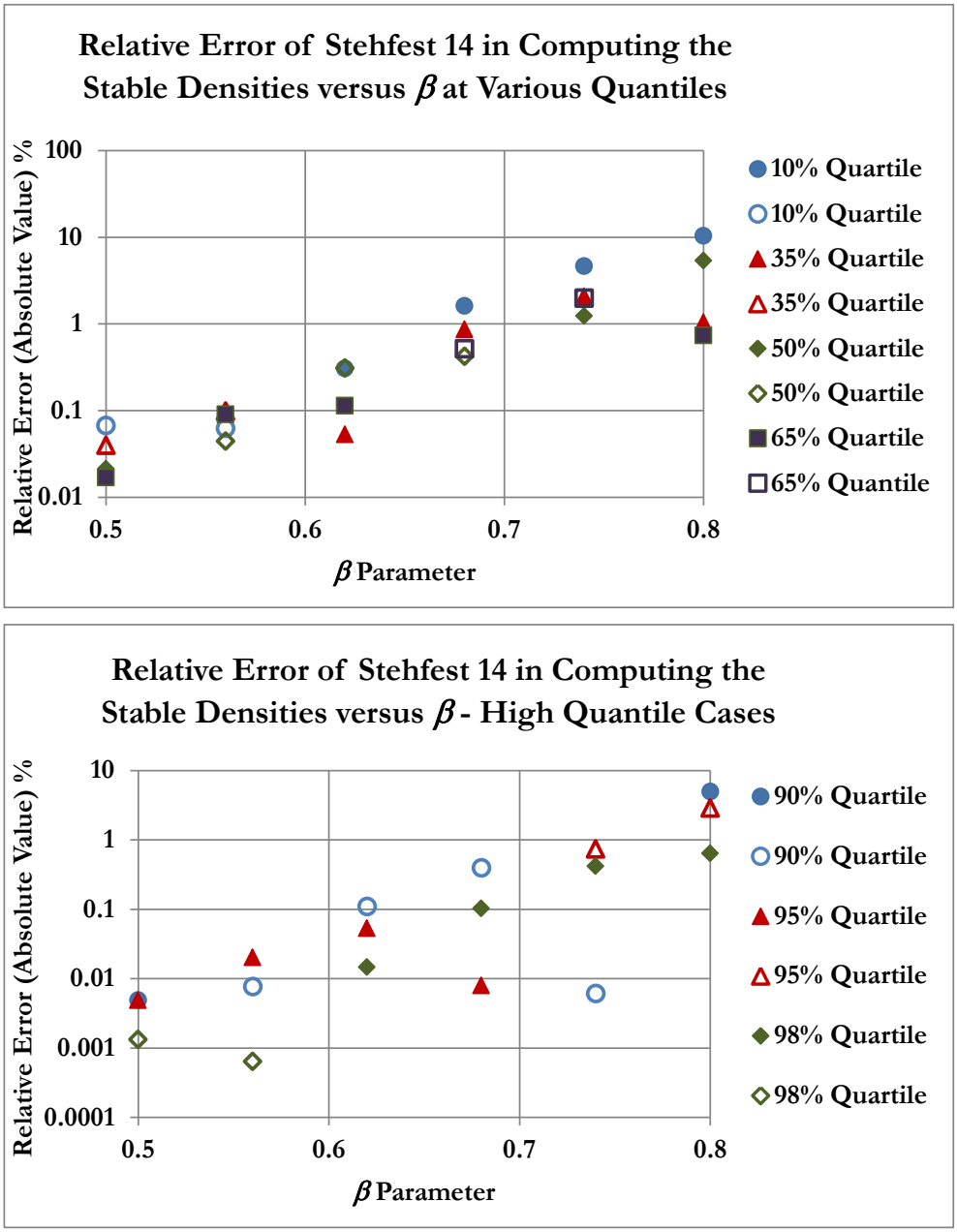

Figure 4.5. Relative Error in the Density $g_\infty(t)$ Computed using the Stehfest Algorithm at Various Quantiles of the Asymptotic Stable Distribution $G_\infty(t)$ (a) 10%, 35%, 50% & 65% Quantiles. (b) 90%, 95% & 98% Quantiles. Filled and Open Symbols Denote the Sign of the Relative Error (+ve or –ve Respectively).

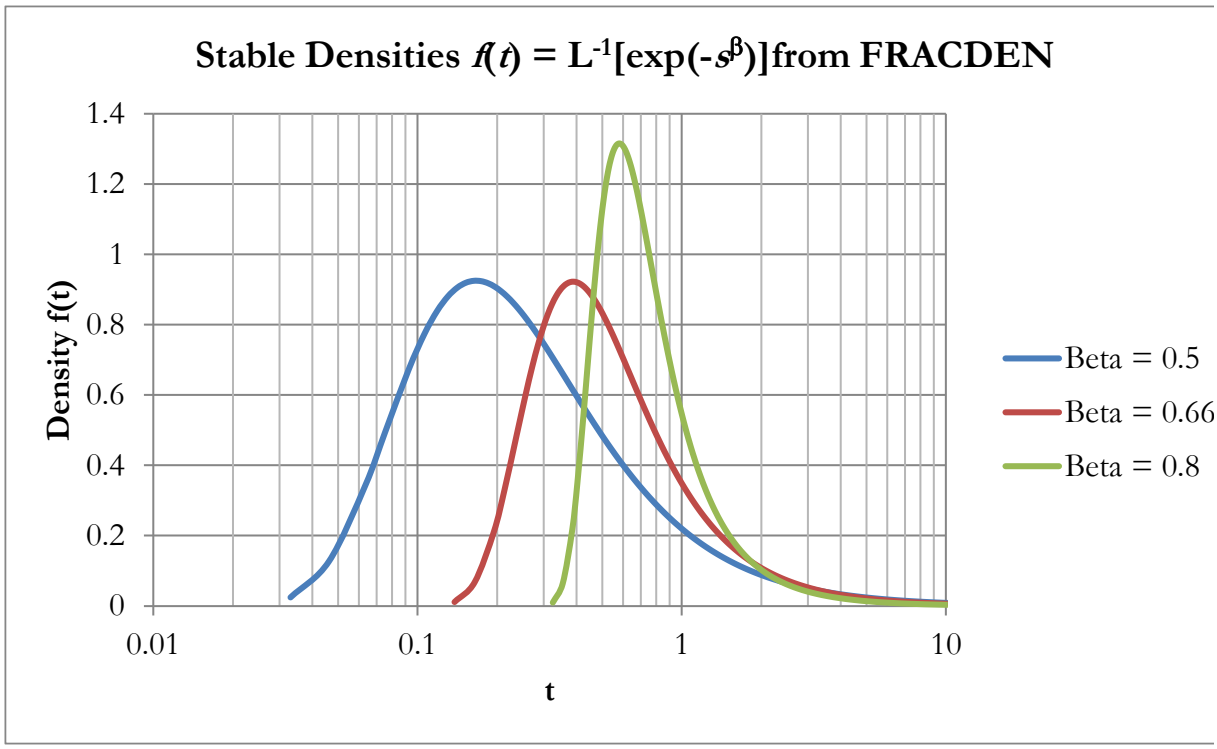

Figure 4.6. The asymptotic stable densities $g_\infty(t)$ for $\beta = 0.5$, 0.66 and 0.8.

4.3 Application to Sums of Long-Tailed "Pareto-Like" Variables

4.3.1 Introduction – A Long-Tailed Distribution with Infinite Variance and Mean for which Statistical Properties of the Sum of Arbitrary Numbers of Samples May be Directly Computed

The final test case treated in this chapter is to sums of long-tailed variables having infinite variance and mean with a density chosen in such a way that the Stehfest algorithm can be directly validated by independent direct calculation.

In this case t_1, t_2 … t_N are IID random variable drawn from a distribution with density $g(t)$, such that

$$\tilde{g}(s) = \frac{1}{1+\sqrt{s}} \tag{4.7}$$

In this case we consider the normalized sum

$$\tau_S = \sum_{i=1}^{N} t_i / N^2 \tag{4.8}$$

and denote the density of τ_S by $g_N(\tau_S)$. Taking the Laplace transform with respect to the normalized sum, we have (*cf* Eq. 2.8):

$$\tilde{g}_N(s) = \int_0^\infty d\tau_S \, f_N(\tau_S) \exp(-s\tau_S) = \int_0^\infty dt_1 ... dt_N \prod_{i=1}^{N} g(t_i) \exp(-st_i / N^2)$$

$$= \frac{1}{(1+\sqrt{s}/N)^N} \tag{4.9}$$

Note that on taking the limit $N \to \infty$ on the right-hand side of Eq. (4.9) we recover the asymptotic stable density of Eq. (2.21) with $\gamma = 1$ and $\beta = ½$.

In order to obtain an explicit expression for $g(t)$, we first note that

$$\tilde{g}(s) = \int_0^\infty du \exp\{-(1+\sqrt{s})u\} \tag{4.10}$$

and then make use of the identity

$$\exp(-2\sqrt{ab}) = \sqrt{\frac{b}{\pi}} \int_0^\infty dt t^{-3/2} \exp(-at - b/t) \tag{4.11}$$

with $a = s$ and $b = u^2/3$. This yields

$$\exp(-\sqrt{s}u) = \frac{u}{2\sqrt{\pi}} \int_0^\infty dt t^{-3/2} \exp\{-st - u^2/(4t)\} \tag{4.12}$$

Substituting Eq. (4.9) back into Eq. (4.7) and changing the order of integration allows us to deduce that

$$g(t) = \frac{1}{2\sqrt{\pi} t^{3/2}} \int_0^\infty du u \exp\{-u - u^2/(4t)\} \tag{4.13}$$

The right-hand side of Eq. (4.10) may be expressed in terms of error functions. First we note that

$$\int_0^\infty du u \exp\{-u - u^2/(4t)\} = \int_0^\infty du\{u + 2t\} \exp\{-u - u^2/(4t)\} - 2t \int_0^\infty du \exp\{-u - u^2/(4t)\} \tag{4.14}$$

The first term on the right-hand side of Eq. (4.14) may be integrated explicitly to obtain

$$\int_0^\infty du\{u + 2t\} \exp\{-u - u^2/(4t)\} = \left[-2t \exp\{-u - u^2/(4t)\}\right]_0^\infty = 2t \tag{4.15}$$

In the second term, we write

$$u + u^2/(4t) = (u + 2t)^2/(4t) - t \tag{4.16}$$

Then $$\int_0^\infty du \exp\{-u - u^2/(4t)\} = \exp(t) \int_{2t}^\infty dv \exp\{-v^2/(4t)\} = \exp(t) 2\sqrt{t} \int_{\sqrt{t}}^\infty dw \exp\{-w^2\} \tag{4.17}$$

In writing Eq. (4.17) we have made use of the successive transformations

$$v = u + 2t; w = 2\sqrt{t}v \tag{4.18}$$

It follows that

$$g(t) = \frac{1}{\sqrt{\pi t}} - \exp(t) \mathrm{erfc}(\sqrt{t}) \tag{4.19}$$

where erfc(x) denotes the complementary error function of x. A key observation, and the reason for the choice of Eq. (4.4), is that a closed-form expression, involving only a single integral, can also be obtained for $g_N(\tau_S)$. We make use of the result

$$\int_0^\infty du u^{N-1}\exp(-au) = \Gamma(N)/a^N = (N-1)!/a^N \tag{4.20}$$

and set a equal to $N + \sqrt{s}$ to write Eq. (4.9) in the form

$$\tilde{g}_N(s) = \frac{N^N}{(N-1)!}\int_0^\infty du u^{N-1}\exp(-Nu)\exp(-\sqrt{s}u) \tag{4.21}$$

Substituting Eq. (4.12) into Eq. (4.21), and reversing the order of integration, we deduce that

$$g_N(\tau_S) = \frac{N^N}{(N-1)!}\frac{1}{2\sqrt{\pi}\tau_S^{3/2}}\int_0^\infty du u^N \exp\{-Nu - u^2/(4\tau_S)\} \tag{4.22}$$

Methods of evaluating the expression on the right-hand side of Eq. (4.22) are discussed in subsection 4.3.3.

4.3.2 Comparison of g(t) with a Shifted Pareto Distribution with β = ½

In this subsection we briefly compare Eq. (4.19) with the shifted Pareto density of Eq. (2.6), where β = ½. Both densities have a tail falling off as $1/t^{3/2}$ for large t, but Eq. (4.16) diverges as $1/t^{1/2}$ for small t while Eq. (2.6) tends to a constant (1/2). This is shown in Figure 4.7. The corresponding distributions are shown in Figure 4.8. The shifted Pareto distribution corresponding to the density given in Eq. (2.6) increases linearly with the parameter t at small values, while the distribution corresponding to Eq. (4.19) rises as $t^{1/2}$.

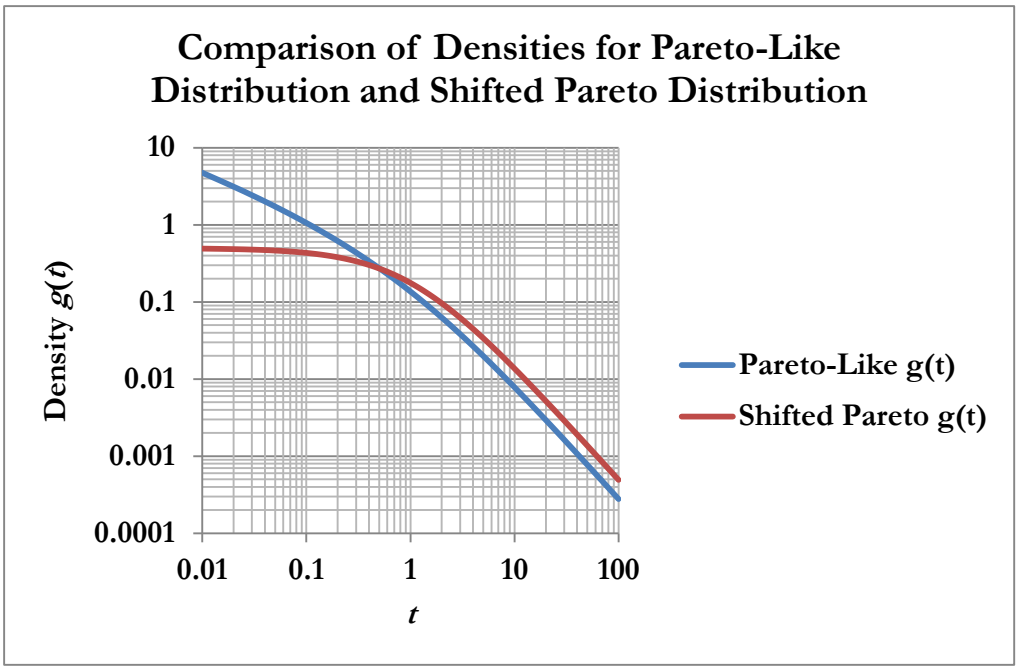

Figure 4.7. Comparison of the Densities Given in Eqs. (4.16) and (2.6) ("Pareto-Like" and "Shifted Pareto" Respectively)

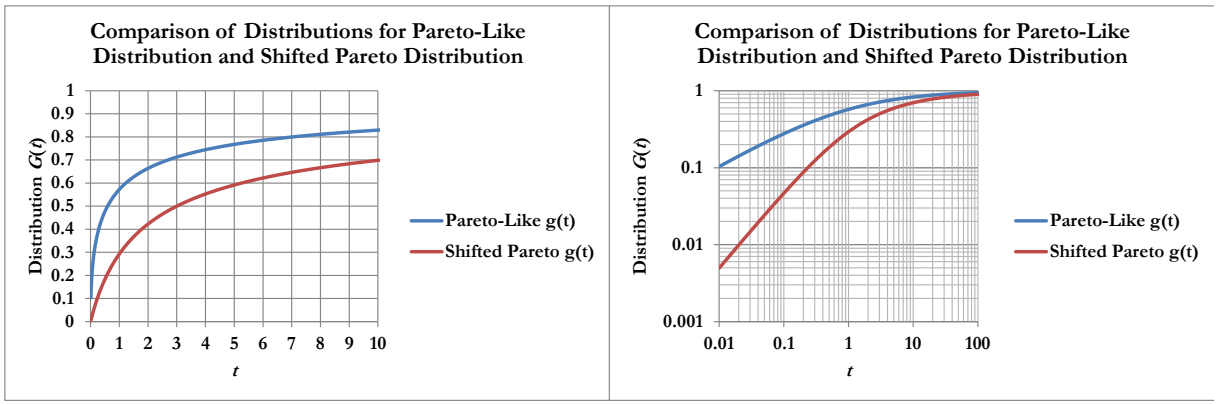

Figure 4.8. Comparison of the Distributions Corresponding to the Densities Given in Eqs. (4.16) and (2.6) ("Pareto-Like" and "Shifted Pareto" Respectively) (a) Linear Scale, (b) Log-Log Plot.

4.3.3 Evaluation of Eq. (4.22)

Developing the right-hand side of Eq. (4.22) as an expansion in powers of τ_S^{-1}, we have

$$g_N(\tau_S) = \frac{1}{2\sqrt{\pi}} \sum_{k=0}^{\infty} \left(-\tfrac{1}{4}\right)^k C_{Nk} \tau_S^{-(3/2+k)} / k! \tag{4.23}$$

with $C_{N0} = 1; C_{Nk} = \prod_{j=1}^{2k} (1 + j/N)$ (4.24)

The series on the right-hand side of Eq. (4.22) is to be interpreted only in a formal sense as it diverges for all τ_S. However, truncating it at the smallest term can give very accurate results, especially for large N. The corresponding direct series may be obtained by writing

$$g_N(\tau_S) = \frac{N^N}{(N-1)!} \frac{1}{2\sqrt{\pi}\tau_S^{3/2}} \sum_{k=0}^{\infty} (-1)^k A_{Nk}(\tau_S) / k! \tag{4.25}$$

with $A_{Nk}(\tau_S) = N^k \int_0^{\infty} du u^{k+N} \exp\{-u^2/(4\tau_S)\}$ (4.26)

We make the following change of variable:

$$w = u^2/(4\tau_S); dw = udu/(2\tau_S); u = 2\sqrt{\tau_S w} \tag{4.27}$$

Then $A_{Nk}(\tau_S) = 2\tau_S N^{-(N-1)} (2N\sqrt{\tau_S})^{k+N-1} \int_0^{\infty} dw w^{(k+N-1)/2} \exp(-w)$

$$= 2\tau_S N^{-(N-1)} (2N\sqrt{\tau_S})^{(k+N-1)} \Gamma\{(k+N+1)/2\} \tag{4.28}$$

Substituting Eq. (4.24) back into Eq. (4.21) we obtain

$$g_N(\tau_S) = \frac{N}{(N-1)!} \frac{1}{\sqrt{\pi\tau_S}} \sum_{k=0}^{\infty} (-1)^k (2N\sqrt{\tau_S})^{(k+N-1)} \Gamma\{(k+N+1)/2\} / k! \tag{4.29}$$

The sum on the right-hand side of Eq. (4.25) converges for all values of the parameter $2N\sqrt{\tau_S}$ but is subject to rounding error if this parameter is too large, as also discussed below Eq. (2.17).

Finally, Eq. (4.18) can be expressed in terms of error functions for all N, though the resulting expressions are only useful for computational purposes for N up to about 5. This is discussed in more detail in Appendix A.

4.3.4 Validation of the Stehfest Algorithm using Eq. (4.21)

Here we describe the comparison between applying Stehfest inversion to Eq. (4.6) versus direct computation using Eq. (4.21). The results shown in Figure 4.9 compare the distribution function calculated using the two methods for low, intermediate and large values of the parameter $\tau_S = t$ (0.1, 1 and 10 respectively). The results are displayed as functions of N up to $N = 100$. The corresponding relative errors in the Stehfest inversion, using a small number of nodes (8), is shown in Figure 4.10 and is seen to be within 0.1% of the direct computation for $t = 1$ and 10, and within about 1% for $t = 0.1$.

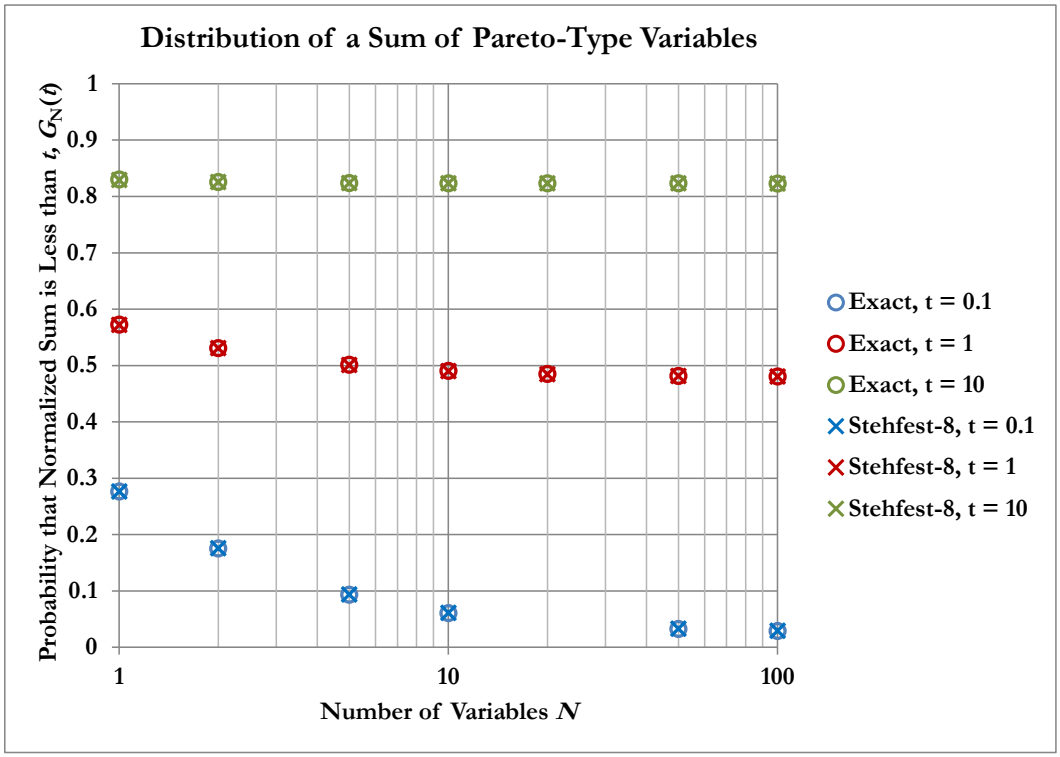

Figure 4.9. Comparison of Stehfest Inversion with Direct Computation for $G_N(t)$ as a Function of N for Small, Intermediate and Large Values of the Parameter t.

Finally, the reduction of relative error on increasing the number of nodes used in the Stehfest inversion is illustrated for $N = 10$ in Figure 4.11.

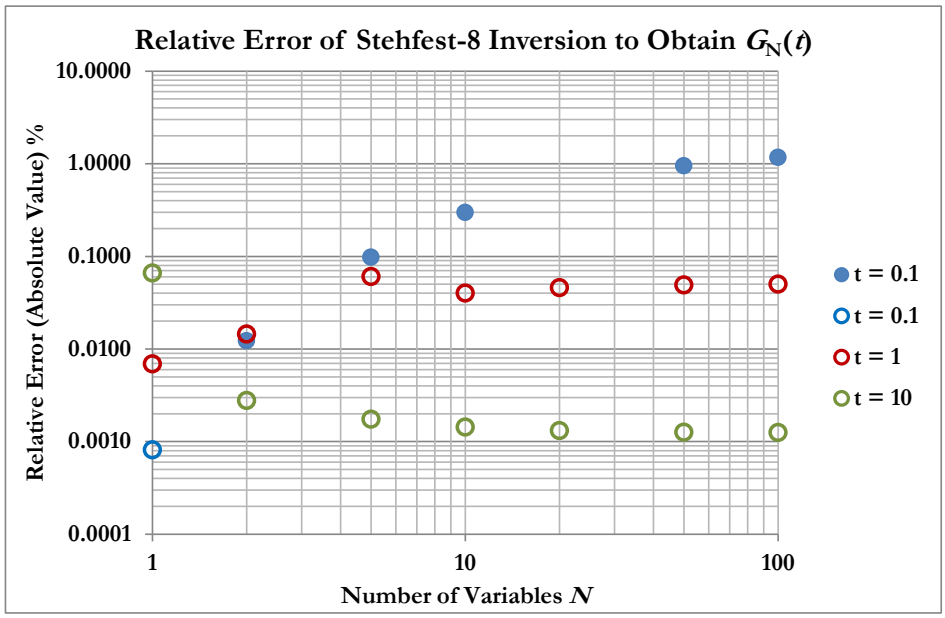

Figure 4.10. Relative Errors in the Stehfest Inversion shown in Figure 4.9. As in Previous Figures Displaying the Relative Error, Filled and Open Symbols Denote a Positive or Negative Relative Error Respectively.

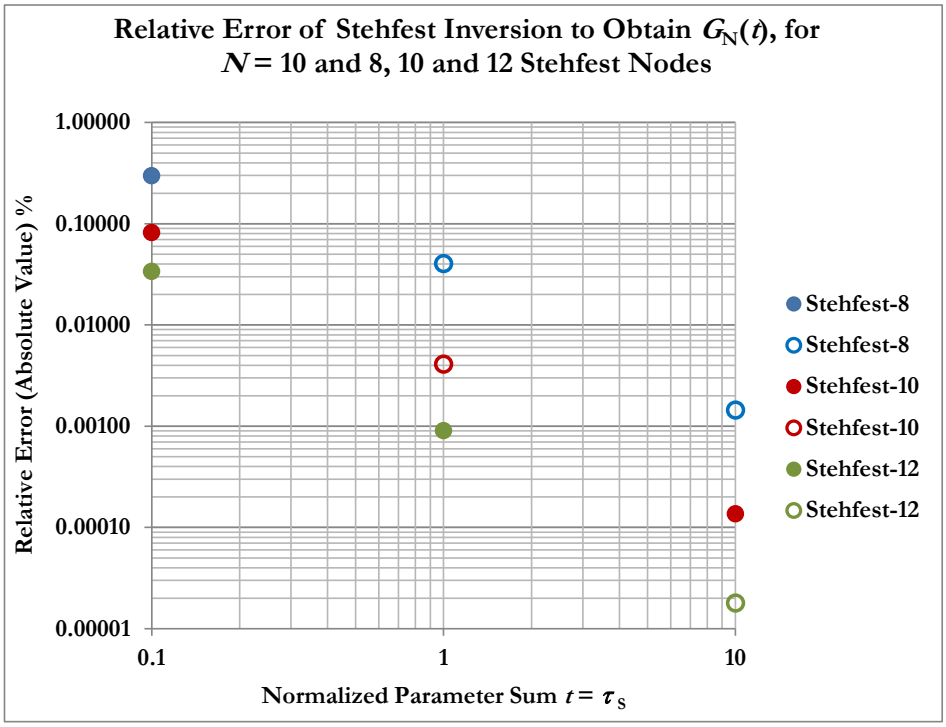

Figure 4.11. Illustration of the Decrease in Relative Errors in the Stehfest Inversion with Increasing Number of Nodes Used.

5. Quantiles of Pareto Sums – Comparison with Literature Results

5.1 Introduction

We saw in the previous chapter, in Section 4.3, that the Stehfest inversion algorithm yielded accurate results for the statistics of sums of long-tailed variables, with a distribution chosen so that these statistics could readily be independently computed. In this chapter, we return to Pareto sums, and compare the results of Stehfest inversion with extensive Monte-Carlo simulations described in [2]. The density and distribution of a sum of N samples drawn from a shifted Pareto distribution, and normalized by dividing by N^{α} is given by

$$g_N(T_N) = L^{-1}\left[\{\tilde{g}(s/N^{\alpha}\}^N\right] \tag{5.1}$$

and $$G_N(T_N) = L^{-1}\left[s^{-1}\{\tilde{g}(s/N^{\alpha}\}^N\right] \tag{5.2}$$

where the Stehfest algorithm described in Chapter 3 is used to perform the inversion operation represented by the operator $L^{-1}[\ldots]$ in Eqs. (5.1) and (5.2). 14 nodes were used for the Stehfest inversion. In order to obtain results for a specific quantile q, where

$$q = G_N(T_N) \tag{5.3}$$

the inversion was performed repeatedly for trial values of T_N until the result matched the desired quantile. This was done using a spreadsheet, but of course could be more efficiently accomplished by writing a computer program. The parameter $\alpha = 1/\beta$ where β is the Pareto parameter (see e.g. Eq. 2.6), and three expressions were used to compute $\tilde{g}(s)$, given in Eqs. (2.13), (2.17) and (2.19), reproduced for convenience as Eqs. (5.4), (5.5) and (5.5) respectively

$$\tilde{g}(s) = 1 - e^s s^{\beta}\Gamma(1-\beta)\Gamma_C(1-\beta, s) \tag{5.4}$$

$$\tilde{g}(s) = 1 - \left\{\Gamma(1-\beta)s^{\beta} - \sum_{n=0}^{\infty}\frac{(-1)^n s^{n+1}}{n!(n+1-\beta)}\right\}\exp(s) \tag{5.5}$$

and $$\tilde{g}(s) = \sum_{n=1}^{\infty}(-1)^{n-1}\frac{\Gamma(n+\beta)}{\Gamma(\beta)s^n} \tag{5.6}$$

The gamma function Γ appearing in Eqs. (5.4)-(5.6) and complementary incomplete gamma function Γ_C appearing in Eq. (5.4) are defined in Eqs.(2.14) and (2.15). The vast majority of results in the present report were obtained using Microsoft Excel, and either (5.5) or (5.6) were used to compute $\tilde{g}(s)$. Some results were obtained using the Python scientific language, which has Γ_C available as a special function, and in this case Eq. (5.4) was used. The shifted, normalized Pareto sum T_N is converted back to the unshifted normalized sum X_N using the relation (see Eq. 2.7)

$$X_N = T_N + N^{(1-\alpha)}$$
(5.7)

The corresponding unnormalized sum $X_N^{(U)}$ is then given by

$$X_N^{(U)} = N^{\alpha} X_N \tag{5.8}$$

5.2 Comparison of Stehfest Algorithm Quantiles with Monte-Carlo Simulation Results

Values of $X_N^{(U)}$ corresponding to certain quantiles were computed using Monte-Carlo simulation in [2] and some results were shown in Table 2 in [2] for N = 2, 5, 10, 20, 50 and 100, and for the 2%, 50% (median) and 98% quantiles. We now compare these results with those obtained by applying the Stehfest algorithm for β = ½ and β = 2/3. Table 5.I (a) shows a side-by-side comparison for β = 1/2, while Table 5.I (b) displays the relative error of the Stehfest result assuming that the Monte-Carlo results are exact. Corresponding results for β = 2/3 are shown in Table 5.2.

Table 5.1 (a). Comparison of Quantiles of Unnormalized Pareto Sums with $\beta = 1/2$ Computed Using Monte-Carlo Simulations and Using the Stehfest Inversion Algorithm.

N	2% Quantile		50% Quantile		98% Quantile	
	MC [2]	Stehfest	MC [2]	Stehfest	MC [2]	Stehfest
2	2.50	2.50	14.94	14.93	10000.17	9999.00
5	10.32	10.31	89.24	89.15	62436.65	62489.75
10	34.92	34.94	351.03	350.96	249338.20	249953.59
20	127.78	127.71	1392.25	1392.50	1004949.00	999799.50
50	753.85	754.24	8654.80	8660.43	6237558.00	6248725.25
100	2960.02	2959.21	34628.25	34584.72	25040967.00	24994769.23

Table 5.1 (b). Relative Error in Percent of the Stehfest Inversion Algorithm for Sums of N Pareto Variables with β = ½.

N	2% Quantile	50% Quantile	98% Quantile
2	0.00	-0.08	-0.01
5	-0.07	-0.10	0.09
10	0.05	-0.02	0.25
20	-0.06	0.02	-0.51
50	0.05	0.07	0.18
100	-0.03	-0.13	-0.18

Table 5.II (a). Comparison of Quantiles of Unnormalized Pareto Sums with $\beta = 2/3$ Computed Using Monte-Carlo Simulations and Using the Stehfest Inversion Algorithm.

N	2% Quantile		50% Quantile		98% Quantile	
	MC [2]	Stehfest	MC [2]	Stehfest	MC [2]	Stehfest
2	2.36	2.36	8.63	8.63	1012.34	1011.19
5	8.44	8.44	37.29	37.26	4029.96	4027.82
10	24.14	24.13	111.27	111.15	11406.04	11425.91
20	71.32	71.28	327.36	327.49	32489.67	32370.97
50	302.14	302.00	1345.80	1344.88	128040.70	128106.54
100	896.63	895.84	3882.27	3870.02	363796.40	362511.28

Table 5.II (b). Relative Error in Percent of the Stehfest Inversion Algorithm for Sums of N Pareto Variables with $\beta = 2/3$.

N	2% Quantile	50% Quantile	98% Quantile
2	0.00	0.00	-0.11
5	0.00	-0.08	-0.05
10	-0.04	-0.11	0.17
20	-0.06	0.04	-0.37
50	-0.05	-0.07	0.05
100	-0.09	-0.32	-0.35

In fact, the Monte-Carlo results quoted in [2], and reproduced in Tables 5.1 and 5.2 are not accurate to the number of places declared, even with the 10^7 realisations used. This can be tested by comparing the quoted results for $\beta = ½$, $N = 2$ with the exact solution. Denoting $X_2^{(U)}$ by x_S we have (see Appendix B)

$$F(x_S) = 1 - 2\sqrt{x_S - 1}/x_S \,;\; x_S \geq 2 \tag{5.9}$$

This equation may readily be solved to obtain an expression for x_S in terms of the quantile $q = F(x_S)$. The result is

$$x_S = 2\omega\left\{\omega + \sqrt{\omega^2 - 1}\right\} \tag{5.10}$$

with $\omega = 1/(1-q)$ (5.11)

For the q = 0.02 (2%) quantile, Eqs. (5.10) and (5.11) allow us to understand why x_S is so close to 10000. Eq (5.10) may be rewritten as

$$x_S = 2\omega\left\{2\omega - (w - \sqrt{\omega^2 - 1})\right\} = 2\omega\left\{2\omega - \frac{1}{\omega + \sqrt{\omega^2 - 1}}\right\} \quad (5.12)$$

For q = 0.02, ω is 50 so we see that the right-hand side of Eq. (5.12) is very close to 9999. This shows a 0.01% error in the Monte-Carlo result. For q = 0.5, $x_S = 8+4\sqrt{3}$ which rounds off to 14.93 rather than 14.94, so if the quoted result is not a typographical error, the error in the Monte-Carlo result is about 0.07%. x_S for q = 0.02 is indeed 2.50 to two decimal places.

The main purpose of [2] is to develop approximations for quantiles of Pareto sums and one of these is the quantile of the corresponding stable density. The quality of this approximation as N increases for $\beta = 2/3$ is shown in Figure 5.1, which is reproduced from [2] (it is Figure 4 (a) of that reference). The results of applying the Stehfest algorithm are superimposed as coloured symbols. The agreement is excellent, as could already be expected from the results in Table 5.II.

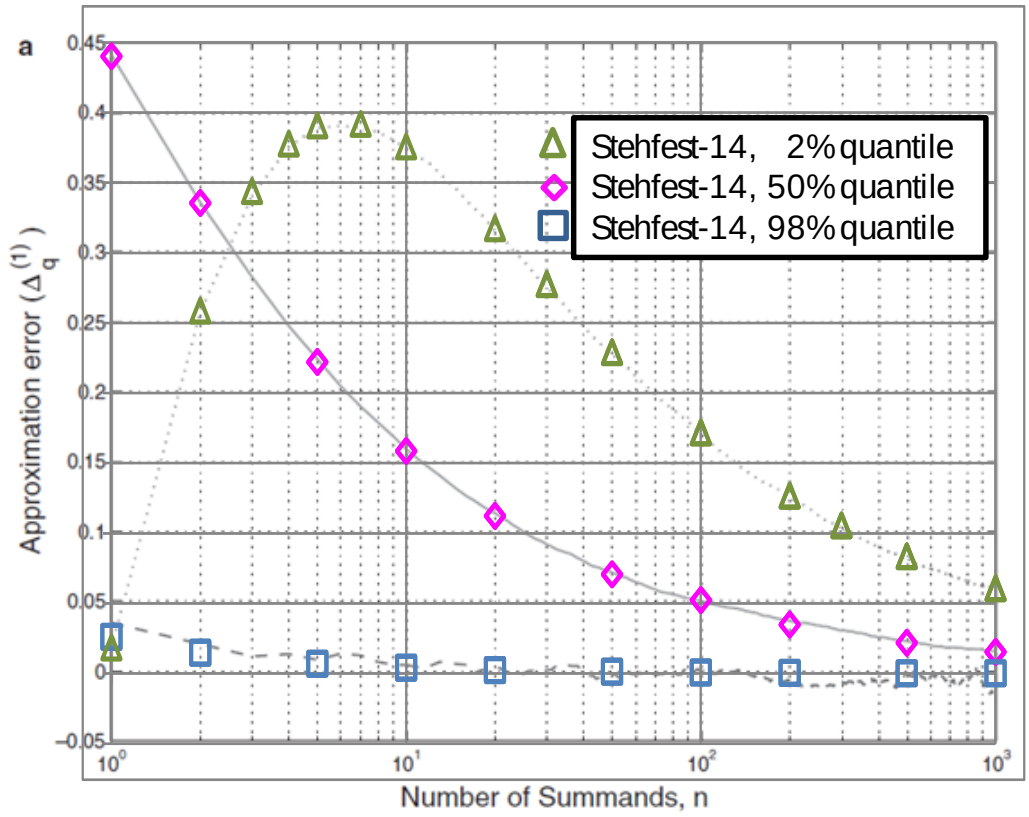

Figure 5.1. *Curves Depict the Approximation Error of the Stable Density Quartile as a Quartile for a Finite Number of Summands N and are Taken from Figure 4a of [2]. Coloured Symbols Show the Results of Applying the Stehfest Algorithm.*

With regard to statistical error in the Monte-Carlo simulation approach, note that statistical fluctuations in the simulation results are clearly visible for the 98% quartile.

5.3 Use of the Stehfest Algorithm to Develop Approximate Expressions for Pareto Sum Quantiles

Since the Stehfest algorithm allows quantiles of the sum of an arbitrary number of samples of Pareto distributed variables to be computed with high accuracy, it can be used to investigate the approach of the suitably normalized sum to the asymptotic stable density parameter. This is done here for the 2%, 50% and 98% quantiles. For the power law exponent $\beta = 2/3$, the deviation of X_N from X_∞ is fitted as a polynomial in $1/N^{1/2}$. The rationale behind this is explained in the theoretical developments of the next section, which contains a general development valid for $0 < \beta < 1$. The fit is as follows:

$$X_\infty - X_N = a_1 / N^{1/2} + a_2 / N + a_2 / N^{3/2} + a_4 / N^2 \tag{5.13}$$

Figure 5.2 shows a plot of X_∞ - X_N, where X_N is computed using the Stehfest algorithm, versus $1/N^{1/2}$, together with polynomial fits in $1/N^{1/2}$ of the form shown in Eq. (5.1). This is done for the 2%, 50% and 98% quartiles.

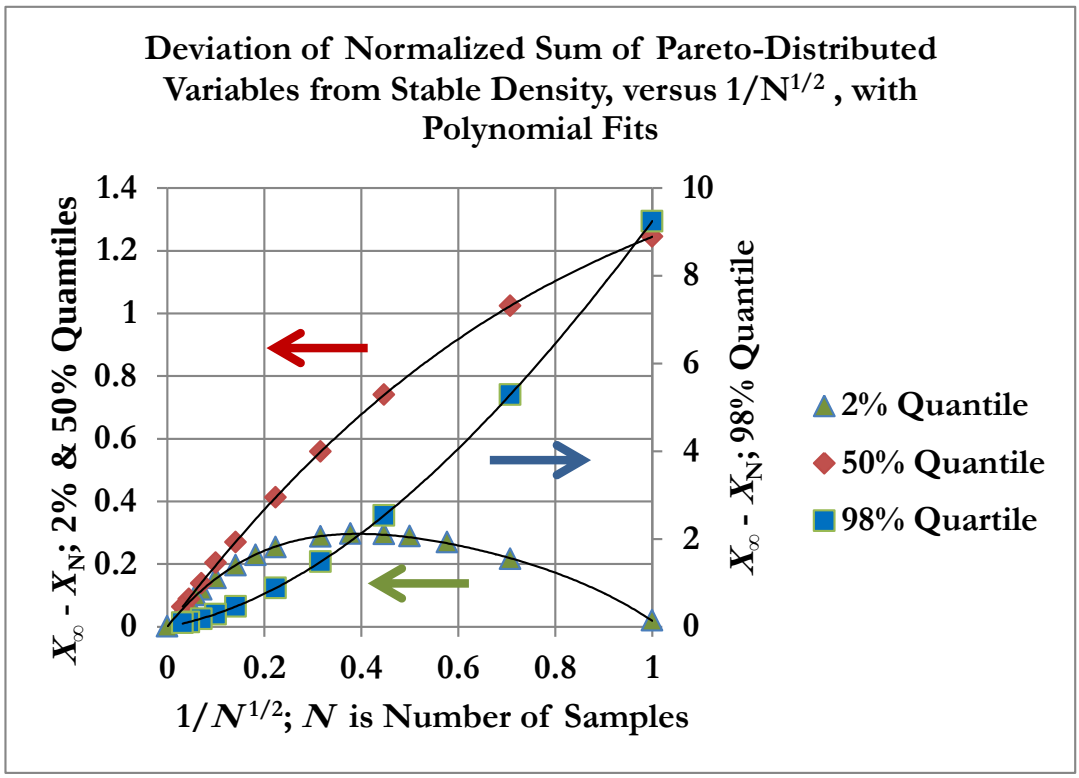

Figure 5.2. Values of X_∞ - X_N for the 2%, 50% and 98% Quantiles versus $1/N^{1/2}$. Polynomial Fits in $1/N^{1/2}$ of the form Given in Eq. (5.13) are also Shown

Values of the coefficients in the polynomial fit are listed in Table 5.III.

Table 5.III Values of the Coefficients of the Fitted Expression for X_∞ - X_N Given in Equation 5.13.

Quantile	Coefficient of Polynomial Expression in Eq. (5.13)			
	a_1	a_2	a_3	a_4
2%	1.9166	-4.2267	3.8125	-1.4835
50%	2.0473	-0.9149	0.0519	0.0603
98%	2.0159	9.0316	-1.9539	0.1522

Note that the coefficient a_1 is close to 2 in all cases. We show theoretically in the next section that it is exactly 2, and also derive an expression for a_2 in terms of the parameter X_∞ and the stable dentity and its derivative evaluated at X_∞. The accuracy of the fitted expression in Eq. (5.13), using the values of the coefficients displayed in Table 5.III is tabulated in Table 5.IV. The magnitude of the relative error is less than 0.4% in all cases.

Table 5.IV. Accuracy of the Polynomial Expression in Eq. (5.13) in Predicting the Value of X_N for Various Numbers of Samples and for the 2%, 50% and 98% Quantiles. Numbers Given are the Relative Error of the Expression in Percent.

N	**2% Quantile**	**50 % Quantile**	**98% Quantile**
1	2.67E-02	8.94E-04	3.37E-05
2	-3.67E-01	-4.12E-03	-9.66E-05
5	2.08E-01	1.49E-02	2.57E-04
10	-2.98E-01	-1.42E-03	-9.59E-07
20	-3.98E-01	-3.11E-02	-1.33E-05
50	-1.12E-01	-5.86E-02	-2.64E-04
100	1.17E-01	1.92E-01	-5.30E-04
200	2.68E-01	-5.99E-02	-1.28E-03
500	3.63E-01	-4.79E-02	-8.88E-04
1000	3.87E-01	-3.80E-02	5.37E-03

The approach used in this section can be used for a larger number of quantiles intermediate between 2% and 98% than just the median in order to develop an expression for the coefficients a_k; $k = 1, 2, 3, 4$, in terms of the quantile q.

5.4 Deductions on Pareto Sum Quantiles from the Structure of the Laplace Transform

In this section we deduce the behaviour of $g_N(t)$ and $G_N(t)$ for small and large values of the parameter t from the structure of the Laplace transform, and also use the properties of the transform to derive a formal asymptotic expansion for the sum of N Pareto-distributed variables X_N for large numbers of samples N.

5.3.1 Behaviour for Small Values of the Parameter

To establish these, we make use of the asymptotic (large s) expansion given in Eq. (5.6) in $\tilde{g}_N(s) = \{\tilde{g}(s/N^\alpha)\}^N$, where $\alpha = 1/\beta$ and invert term-by-term to obtain an expression for $g_N(t)$ for sufficiently small t. We have

$$\tilde{g}_N(s) = \left(\frac{\beta N^\alpha}{s}\right)^N \left\{1 - \frac{(1+\beta)N^\alpha}{s} + \frac{(1+\beta)(2+\beta)N^{2\alpha}}{s^2} + O[(N^\alpha/s)^3]\right\}^N \tag{5.13}$$

Expanding out the braces on the right-hand side of Eq. (A.4) we obtain

$$\tilde{g}_N(s) = \left(\frac{\beta N^\alpha}{s}\right)^N \left\{1 - \frac{(1+\beta)N^{1+\alpha}}{s} + \frac{(1+\beta)N^{2\alpha+1}\{2+\beta+\frac{1}{2}(N-1)(1+\beta)\}}{s^2} + O[(N^{1+\alpha}/s)^3]\right\} \tag{5.14}$$

Simplifying the second term in braces on the right-hand side of Eq. (5.14) we obtain

$$\tilde{g}_N(s) = \left(\frac{\beta N^\alpha}{s}\right)^N \left\{1 - \frac{(1+\beta)N^{1+\alpha}}{s} + \frac{1}{2}\frac{(1+\beta)N^{2\alpha+1}\{N(1+\beta)+3+\beta\}}{s^2} + O[(N^{1+\alpha}/s)^3]\right\} \tag{5.15}$$

Inverting Eq. (5.15) yields the result

$$g_N(t) = \frac{(\beta N^\alpha)^N}{(N-1)!} t^{N-1} \left\{1 - (1+\beta)N^\alpha t + \frac{1}{2}(1+\beta)\frac{N(1+\beta)+3+\beta}{N+1}(N^\alpha t)^2 + O[(N^\alpha t)^3]\right\} \tag{5.16}$$

The terms in braces on the right-hand side of Eq. (5.16) become successively smaller for $N^\alpha t << 1$. On defining $h_N(t)$ as

$$h_N(t) \equiv (N-1)!\, t g_N(t)/(\beta N^\alpha t)^N \tag{5.17}$$

The expansion in Eq. (A.7) may be written as

$$h_N(t) = 1-(1+\beta)N^{\alpha}t+\tfrac{1}{2}(1+\beta)\frac{N(1+\beta)+3+\beta}{N+1}(N^{\alpha}t)^2+O[(N^{\alpha}t)^3] \qquad (5.18)$$

In order to compare Eq. (5.18) with the results of Stehfest inversion, $h_N(t)$ is plotted as a function of $N^{\alpha}t$ in Figure 5.3, for $\beta = 2/3$ and $N = 5$. The quadratic approximation shown on the right-hand side of Eq. (5.18) is accurate to within about 5% up to a value $N^{\alpha}t = 0.3$. Note that the accuracy of the Stehfest inversion algorithm is compromised at small values of the parameter, particularly when the computed density is small. This is shown in Figure 5.4, where the difference between the computations performed using Stehfest-12 and Stehfest-14 is shown, for $N = 7$, in which the computed densities are much lower than for $N = 5$. The Stehfest-14 computations and the quadratic approximation coincide well for the four data points shown.

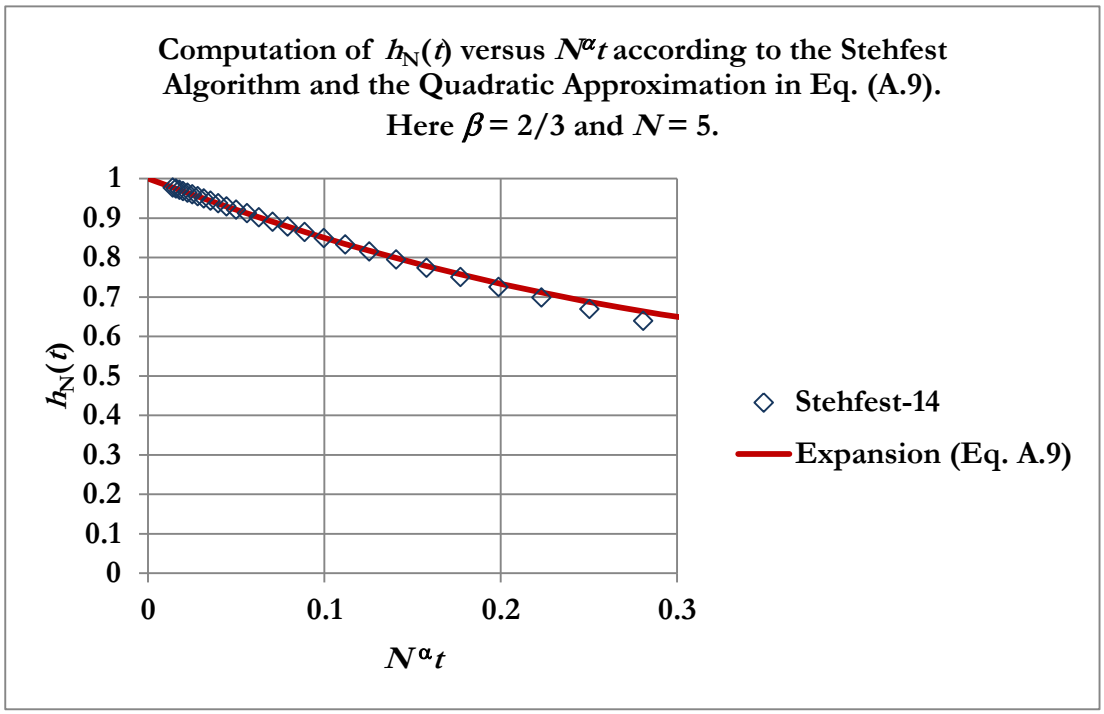

Figure 5.3. Computation of $h_N(t)$ versus $N^{\alpha}t$ According to the Stehfest Algorithm and the Quadratic Approximation in Eq. (5.18). Here $\beta = 2/3$ and $N = 5$.

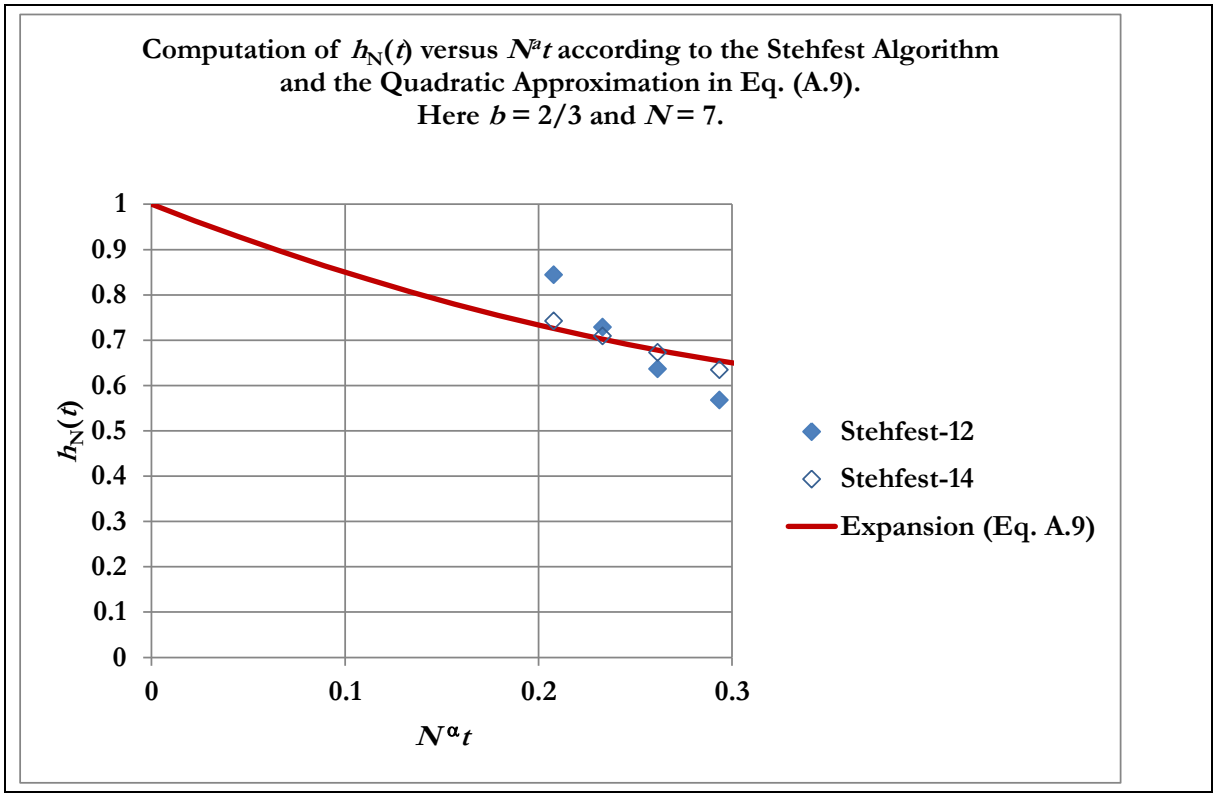

Figure 5.4 *Computation of $h_N(t)$ versus $N^\alpha t$ According to the Stehfest Algorithm and the Quadratic Approximation in Eq. (4.18). Here $\beta = 2/3$ and $N = 7$.*

Eq. (5.16) may readily be integrated to obtain the cumulative distribution function $G_N(t)$. The result is

$$G_N(t) = \frac{(\beta N^\alpha)^N}{N!} t^N \left\{ 1 - (1+\beta)\frac{N}{N+1}(N^\alpha t) + \tfrac{1}{2}(1+\beta)\frac{N(1+\beta)+3+\beta}{N+1}\frac{N}{N+2}(N^\alpha t)^2 + O[(N^\alpha t)^3] \right\} \tag{5.19}$$

Since $t < 0.3/N^\alpha$, Eq. (5.19) is only useful in estimating quantiles for which, rougly speaking.

$$G_N(t) < \frac{(0.3\beta)^N}{N!} \tag{5.20}$$

For $\beta = 2/3$, and considering the 2% quantile (i.e. $G_N(t) = 0.02$), its usefulness is limited to $N = 1$ and 2.

5.3.2 Behaviour for Large Values of the Parameter

In this case we may make use of the small-s expansion for $\tilde{g}(s)$ which is given by

$$\tilde{g}(s) = 1 - \left\{ \Gamma(1-\beta) s^{\beta} - \sum_{n=0}^{\infty} \frac{(-1)^n s^{n+1}}{n!(n+1-\beta)} \right\} \exp(s) \tag{5.21}$$

The form of the function [14-16] allows us to extend the formula

$$L^{-1}[s^{-\nu}] = t^{\nu-1} / \Gamma(\nu) \tag{5.22}$$

to the negative real line and formally evaluate the inverse term by term. Applying this procedure directly to Eq. (5.21), and comparing with the known answer, we make use of the results that

$$L^{-1}[s^{\beta+n}] = \frac{t^{-\beta-n-1}}{\Gamma(-\beta-n)} = \frac{t^{-\beta}(-1/t)^{n+1} \prod_{k=0}^{n} (\beta+k)}{\Gamma(1-\beta)}; \; n = 0, 1, \ldots; \; \beta \text{ nonintegral} \tag{5.23}$$

and $$L^{-1}[s^{n}] = 0; n = 1, 2 \ldots \tag{5.24}$$

Then $$L^{-1}[\tilde{g}(s)] = \frac{\beta}{t^{1+\beta}} - \frac{\beta(\beta+1)}{1! t^{2+\beta}} + \frac{\beta(\beta+1)(\beta+2)}{2! t^{3+\beta}} - \ldots \tag{5.25}$$

This is immediately recognized as the expansion in inverse powers of t of $g(t) = \beta/(1 + t)^{(1+\beta)}$.

Before turning our attention to $g_N(t)$, we address the stable density $g_\infty(t) = L^{-1}[\exp(-s^{\beta})]$. In this case, we need the result

$$L^{-1}[s^{n\beta}] = \frac{t^{-n\beta-1}}{\Gamma(-n\beta)} = \frac{t^{-n\beta-1}(-1)^{m+1} \prod_{k=0}^{m} (n\beta-k)}{\Gamma(m+1-n\beta)}; \; m = [n\beta], \; n\beta - m \neq 0; \; n = 1, 2 \ldots \tag{5.26}$$

$$L^{-1}[s^{n\beta}] = 0; n\beta - m = 0; n = 1, 2, 3 \ldots \tag{5.27}$$

The notation $[n\beta]$ in Eq. (5.26) means the integral part of $n\beta$. Eqs. (5.26) are applicable to the general case of inverting $\exp(-s^{\beta})$. For the specific case of $\beta = 2/3$, which is a simple fraction, it is preferable to group the expansion of $\exp(-s^{2/3})$ into three series, which allows us to apply Eqs. (5.23) and (5.24). This is done as follows

$$\exp(-s^{2/3}) = \left(\sum_{k=0}^{\infty} (-1)^k s^{2k} / (3k)! \right) - \left(\sum_{k=0}^{\infty} (-1)^k s^{2/3+2k} / (3k+1)! \right)$$

$$+\left(\sum_{k=0}^{\infty}(-1)^k s^{4/3+2k}/(3k+2)!\right) \tag{5.28}$$

Application of Eqs. (5.23) and (5.24) then yield the result

$$L^{-1}[\exp(-s^{2/3})] = \frac{1}{\Gamma(1-\beta)}\left\{\frac{\beta}{t^{1+\beta}} - \frac{\beta(\beta+1)(\beta+2)}{4!t^{3+\beta}} + \frac{\prod_{k=0}^{4}(\beta+k)}{7!t^{5+\beta}} - ..\right\}.$$

$$-\frac{1}{\Gamma(1-2\beta)}\left\{\frac{2\beta}{2!t^{1+2\beta}} - \frac{2\beta(2\beta+1)(2\beta+2)}{5!t^{3+\beta}} + \frac{\prod_{k=0}^{4}(2\beta+k)}{8!t^{5+\beta}} - ..\right\}.; \beta = 2/3 \tag{5.29}$$

Making use of the fact that

$$\Gamma(1-2\beta) = \Gamma(2-2\beta)/(1-2\beta) = -\Gamma(2-2\beta)/(2\beta-1) \tag{5.30}$$

Eq. (5.29) may be rewritten as

$$L^{-1}[\exp(-s^{2/3})] = \frac{1}{\Gamma(1-\beta)}\left\{\frac{\beta}{t^{1+\beta}} - \frac{\beta(\beta+1)(\beta+2)}{4!t^{3+\beta}} + \frac{\prod_{k=0}^{4}(\beta+k)}{7!t^{5+\beta}} - ..\right\}.$$

$$-\frac{(2\beta-1)}{\Gamma(2-2\beta)}\left\{\frac{2\beta}{2!t^{1+2\beta}} - \frac{2\beta(2\beta+1)(2\beta+2)}{5!t^{3+2\beta}} + \frac{\prod_{k=0}^{4}(2\beta+k)}{8!t^{5+2\beta}} - ..\right\}.; \beta = 2/3 \tag{5.31}$$

The two series on the right-hand side of Eq. (5.31) are absolutely convergent for all values of t, but for values of t that are too large successive terms become very large before finally diminishing, so that a large number of terms are required to obtain convergence and the result is susceptible to roundoff errors. To test the convergence of Eq. (5.31), we use Eq. (2.23), which for $\gamma = 2$ can be written as

$$g_\infty(t;1) = L^{-1}[\exp(-s^{2/3}] = 2^{3/2} g_\infty(2^{3/2}t;2) \tag{5.32}$$

and then apply Eq. (2.13), which relates $g_\infty(t, 2)$ to a special function, the Whittaker function of the second kind. An online calculator for computing this function can be found in [17]. Figure 5.5 shows the number of terms needed to achieve convergence to nine places of decimals in the series on the right-hand side of Eq. (5.31). The result agrees with the calculations performed using [17] to these nine places, except for the lowest value of t, 0.2, for which roundoff errors have degraded accuracy at the 9th place.

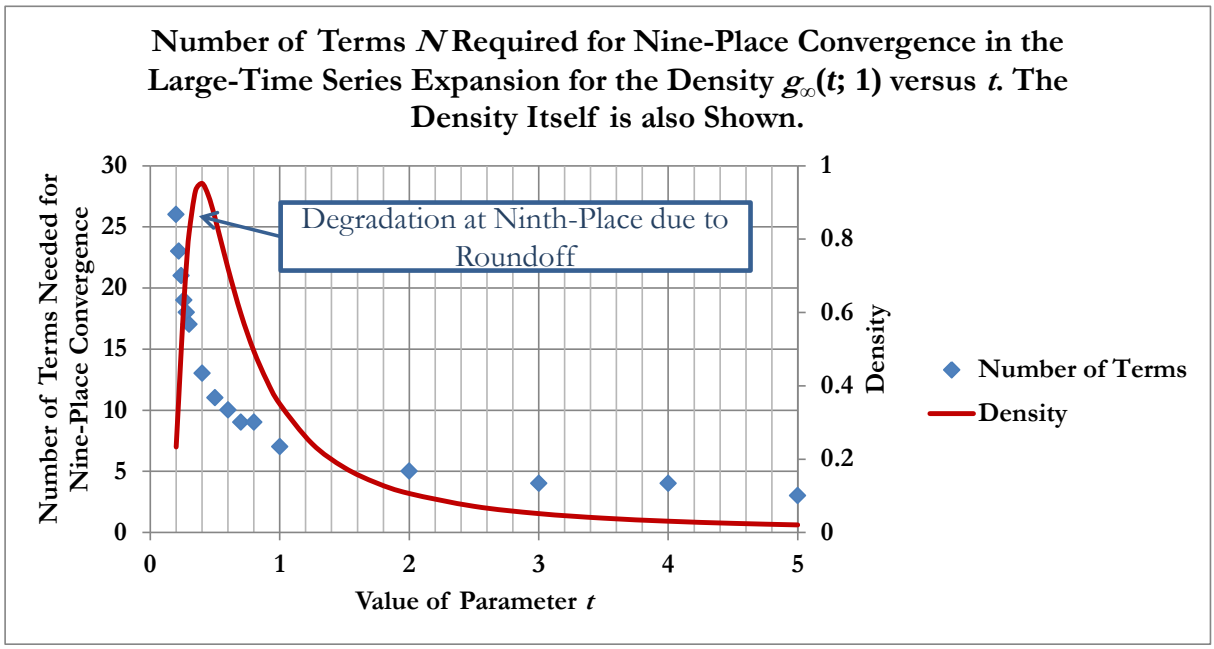

Figure 5.5. For The Two Series on the Right-Hand Side of Eq. (5.31) Each Summed to the Nth Term, the Value of N Required to Achieve Convergence to Nine Decimal Places, as a Function of the Parameter t. The Density $g_\infty(t; 1)$ is Also Plotted.

Note that Eq. (5.31) can still be used for values of t that are below the density mode, in other words its applicability is not restricted to the large parameter tail.

The cumulative distribution function $G_\infty(t; 1)$ corresponding to the density $g_\infty(t; 1)$ may readily be computed using Eq. (5.31) by using the relation

$$G_\infty(t;1) = 1 - \int_t^\infty dt' g_\infty(t';1) \tag{5.33}$$

The right-hand side of Eq. (5.31) can be substituted into Eq. (5.33) and integrated term-by-term. The result is

$$G_\infty(t;1) = 1 - \frac{1}{\Gamma(1-\beta)}\left\{\frac{1}{t^\beta} - \frac{\beta(\beta+1)}{4!t^{2+\beta}} + \frac{\prod_{k=0}^{3}(\beta+k)}{7!t^{4+\beta}} - ..\right\}.$$

$$+\frac{(2\beta-1)}{\Gamma(2-2\beta)}\left\{\frac{1}{2!t^{2\beta}}-\frac{2\beta(2\beta+1)}{5!t^{2+2\beta}}+\frac{\prod_{k=0}^{3}(2\beta+k)}{8!t^{4+2\beta}}-..\right\}.;\beta=2/3 \qquad (5.34)$$

Provided that a sufficient number of terms is used in the computation, and Figure 5.4 provides a guideline to this, an accuracy of at least nine places of decimals should be obtainable using Eq. (5.34), as successive terms in the two series on the right-hand side of Eq. (5.34) do not become as large as the corresponding terms in Eq. (5.31) and ultimately diminish more rapidly.

Moving on to $g_N(t)$, we have

$$\tilde{g}_N(s)=\left[1-\left\{\Gamma(1-\beta)\frac{s^\beta}{N}-\frac{1}{N^\alpha}\sum_{n=0}^{\infty}\frac{(-1)^n s^{n+1}}{n!(n+1-\beta)N^{n\alpha}}\right\}\exp(s/N^\alpha)\right]^N \qquad (5.35)$$

With $\beta = 2/3$, the leading order *non-integral* powers of s appearing in the expansion on the right-hand side of Eq. (5.35) are $s^{2/3}$, $s^{4/3}$, $s^{5/3}$ giving rise to inverse powers of t of $1/t^{5/3}$, $1/t^{7/3}$ and $t^{8/3}$. In general we have

$$\tilde{g}_N(s)=\sum_{n=0}^{\infty}a_n s^{2/3+n}+\sum_{n=1}^{\infty}b_n s^{1/3+n}+\sum_{n=1}^{\infty}c_n s^n \qquad (5.36)$$

with the last summation not contributing to the inverse due to Eq. (5.24). We deduce that

$$a_0=-\Gamma(\tfrac{1}{3});b_1=\tfrac{1}{2}\Gamma^2(\tfrac{1}{3})\left\{1-N^{-1}\right\} \qquad (5.37)$$

and $$a_1=-\Gamma(\tfrac{1}{3})/N^{3/2}-3\Gamma(\tfrac{1}{3})\left\{N^{-1/2}-N^{-3/2}\right\}=-\Gamma(\tfrac{1}{3})\left\{3N^{-1/2}-2N^{-3/2})\right\} \qquad (5.38)$$

Setting $\beta = 2/3$ and $n = 0$ and 1 in Eq. (5.23), we obtain

$$L^{-1}[s^{2/3}]=-\tfrac{2}{3}\frac{t^{-5/3}}{\Gamma(\frac{1}{3})};L^{-1}[s^{5/3}]=\tfrac{10}{9}\frac{t^{-8/3}}{\Gamma(\frac{1}{3})} \qquad (5.39)$$

Similarly, setting $\beta = 1/3$ and $n = 1$ in Eq. (5.23), we obtain

$$L^{-1}[s^{4/3}]==\tfrac{4}{9}\frac{t^{-7/3}}{\Gamma(\frac{2}{3})} \qquad (5.40)$$

Putting everything together, we may write

$$g_N(t)=\tfrac{2}{3}t^{-5/3}+\tfrac{2}{9}\left\{1-N^{-1}\right\}\frac{\Gamma^2(\frac{1}{3})}{\Gamma(\frac{2}{3})}t^{-7/3}-\tfrac{10}{9}\left\{3N^{-1/2}-2N^{-3/2}\right\}t^{-8/3}+O[t^{-10/3}] \qquad (5.41)$$

This obviously yields the correct result for $N = 1$. Proceeding in analogous fashion to Eq. (5.17) we define a function $h_N^{(A1)}(t)$ such that

$$h_N^{(A1)}(t)\equiv\tfrac{3}{2}t^{5/3}g_N(t) \qquad (5.42)$$

Then $$h_N^{(A1)}(t)=1+\tfrac{1}{3}\left\{1-N^{-1}\right\}\frac{\Gamma^2(\frac{1}{3})}{\Gamma(\frac{2}{3})}t^{-2/3}-\tfrac{5}{3}\left\{3N^{-1/2}-2N^{-3/2}\right\}t^{-1}+O[t^{-5/3}] \qquad (5.43)$$

In Figure 5.6, implementation of the Stehfest algorithm is compared with Eq. (5.43) for t in the range 100 to 10000 and for N = 2, 5 and 10. A good comparison is obtained, but we see that, over this range of t, $h_N^{(A1)}(t)$ differs by only a few percent from the first term on the right-hand side of Eq. (5.43), namely unity. A more sensitive comparison can be made by defining a second function $h_N^{(A2)}(t)$ as follows:

$$h_N^{(A2)}(t) \equiv t^{2/3}\left\{h_N^{(A1)}(t) - 1\right\} \tag{5.44}$$

It then follows that

$$h_N^{(A2)}(t) = \tfrac{1}{3}\left\{1 - N^{-1}\right\}\frac{\Gamma^2(\frac{1}{3})}{\Gamma(\frac{2}{3})} - \tfrac{5}{3}\left\{3N^{-1/2} - 2N^{-3/2}\right\}t^{-1/3} + O[t^{-1}] \tag{5.45}$$

Figure 5.7 compares the Stehfest implementation of $h_N^{(A2)}(t)$ versus $t^{1/3}$ with the straight-line approximation on the right-hand side of Eq. (5.45). In this case the comparison is somewhat compromised by the accuracy of the Stehfest-14 approximation for large values of the parameter (Stehfest-12 is also shown in addition to Stehfest -14).

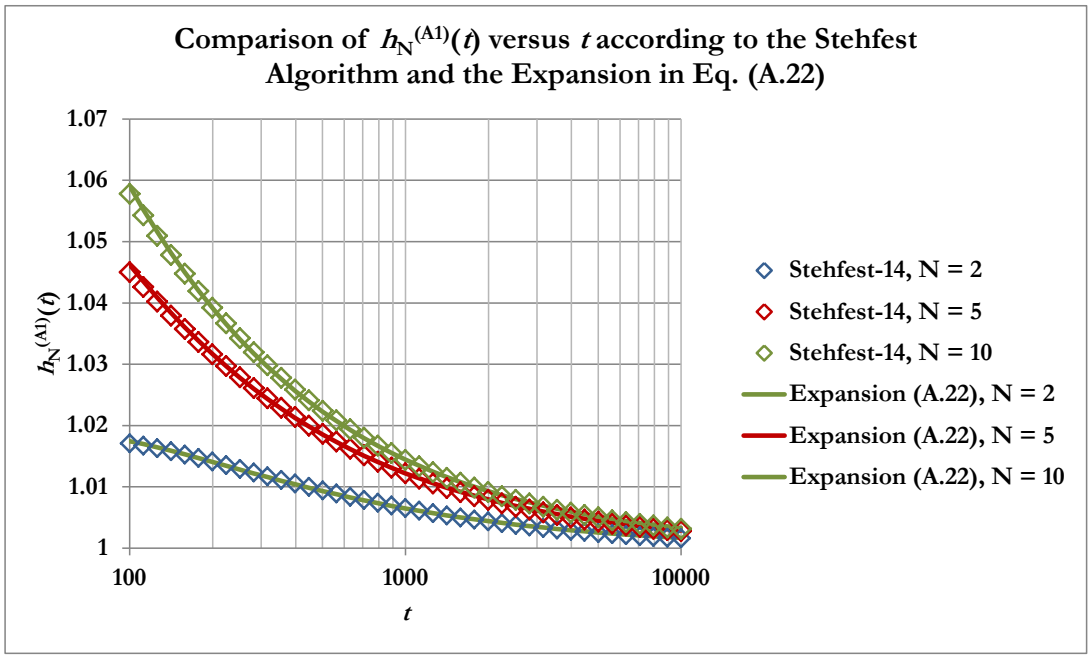

Figure 5.6. Comparison of $h_N^{(A1)}(t)$ versus t Computed by Implementing the Stehfest Algorithm with the Approximation on the Right-Hand Side of Eq. (5.41).

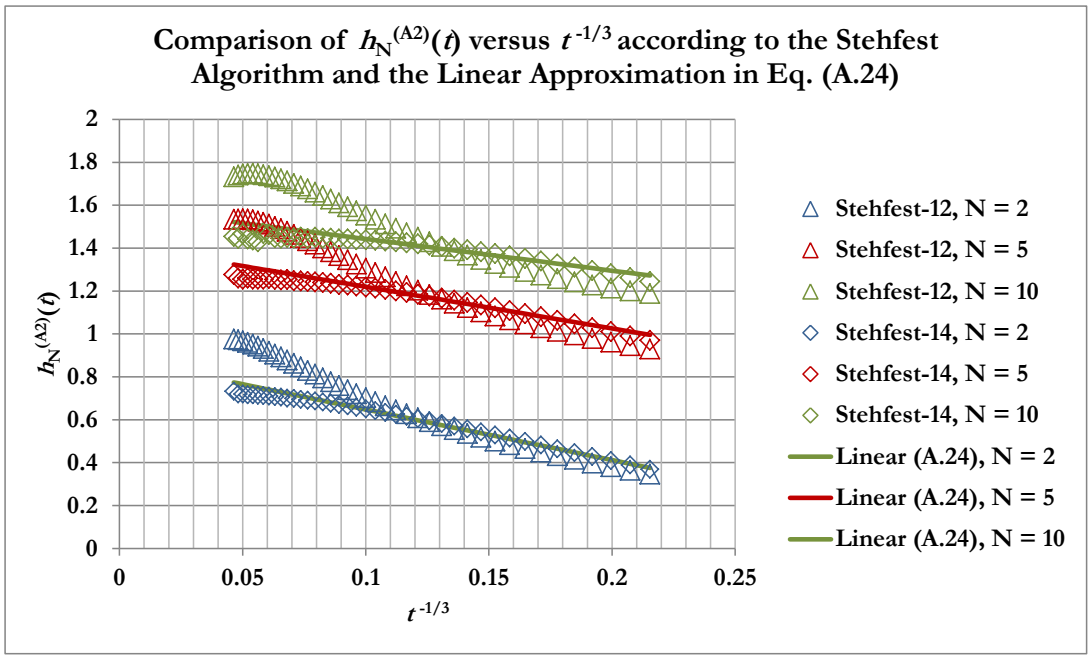

Figure 5.7. *Comparison of $h_N^{(A2)}(t)$ versus $t^{-1/3}$ Computed by Implementing the Stehfest Algorithm with the Linear Approximation on the Right-Hand Side of Eq. (5.43).*

Eq. (5.41) may be integrated to obtain an expression for the complementary cumulative distribution function. We have

$$1-G_N(t)=\int_t^\infty dt' g_N(t') = t^{-2/3} + \tfrac{1}{6}\left\{1-N^{-1}\right\}\frac{\Gamma^2(\frac{1}{3})}{\Gamma(\frac{2}{3})}t^{-4/3} - \tfrac{2}{3}\left\{3N^{-1/2}-2N^{-3/2}\right\}t^{-5/3}+O[t^{-7/3}] \qquad (5.41)$$

For large quantiles, Eq. (5.41) is useful in determining how the parameter for a given quantile depends on N. For example, for $G_N(t) = q = 0.98$ we have, to lowest order in the expansion on the right-hand side of Eq. (5.41),

$$1-q=t^{-2/3} \qquad (5.42)$$

or $$t=(1-q)^{-3/2}=0.02^{-3/2}=250\sqrt{2}=353.56 \qquad (5.43)$$

Denoting the above approximation by t_0 , a better approximation may be obtained by rearranging Eq. (5.41) as

$$1-q==t^{-2/3}\left\{1+\tfrac{1}{6}\left\{1-N^{-1}\right\}\frac{\Gamma^2(\frac{1}{3})}{\Gamma(\frac{2}{3})}t^{-2/3}-\tfrac{2}{3}\left\{3N^{-1/2}-2N^{-3/2}\right\}t^{-1}\right\} \qquad (5.44)$$

Subsequently, Eq. (5.44) is rearranged as

$$t = \left\{1 + \tfrac{1}{6}\left(1 - N^{-1}\right)\frac{\Gamma^2\left(\tfrac{1}{3}\right)}{\Gamma\left(\tfrac{2}{3}\right)}t^{-2/3} - \tfrac{2}{3}\left(3N^{-1/2} - 2N^{-3/2}\right)t^{-1}\right\}^{3/2}(1-q)^{-3/2} \tag{5.45}$$

An improved approximation t_1 can be obtained using Eq. (5.45) by writing

$$t_1 = \left\{1 + \tfrac{1}{6}\left(1 - N^{-1}\right)\frac{\Gamma^2\left(\tfrac{1}{3}\right)}{\Gamma\left(\tfrac{2}{3}\right)}t_0^{-2/3} - \tfrac{2}{3}\left(3N^{-1/2} - 2N^{-3/2}\right)t_0^{-1}\right\}^{3/2}(1-q)^{-3/2} \tag{5.46}$$

Substituting Eq. (5.43) into Eq. (5.46), where we are denoting t in Eq. (5.43) by t_0, we obtain

$$t_1 = \left\{1 + \tfrac{1}{6}\left(1 - N^{-1}\right)\frac{\Gamma^2\left(\tfrac{1}{3}\right)}{\Gamma\left(\tfrac{2}{3}\right)}(1-q) - \tfrac{2}{3}\left(3N^{-1/2} - 2N^{-3/2}\right)(1-q)^{3/2}\right\}^{3/2}(1-q)^{-3/2} \tag{5.47}$$

For q = 0.98, the values of t obtained using the approximation in Eq. (5.47) are compared in Table 5.V with those obtained using the Stehfest algorithm, and from Monte-Carlo simulations in [2].

Table 5.V. Value of the Normalized Sum t of N Samples Drawn from a Shifted Pareto Distribution with β = 2/3 Corresponding to the 98% Quantile.

N	*t*: Eq. (5.47)	*t:* Stehfest Algorithm	*t:* Monte-Carlo [2]*
1	352.55	352.55	
2	356.83	356.8	357.21
5	359.9	359.81	360
10	361.13	361	360.37
20	361.84	361.69	363.02
50	362.35	362.2	362.01
100	362.57	362.41	363.7
200	362.7	362.55	
500	362.81	362.65	
1000	362.86	362.68	

*The figures listed in this column are derived from those presented in the 5th column of Table 5.II (a), which were published in [2], by subtracting N and dividing by $N^{3/2}$.

We note that the values for t obtained from the analytical expression in Eq. (5.41) are very close to those obtained using the Stehfest algorithm, with a relative difference between the two of less than 0.03%.

5.3.3 Large-N Asymptotic Expansions for Quantiles Corresponding to Fixed Values of the Parameter t

In Sections 5.2 and 5.3 we considered how, for fixed quantiles, the value of the parameter t for a normalized sum of N Pareto-distributed variables approaches its stable-distribution value as N increases. We next use a different small-s expansion of Eq. (5.35) to show this behaviour for the quantiles for fixed values of the parameter t, and establish explicit expressions for coefficients in the large-N asymptotic expansion in terms of the stable density and its derivatives. We take the logarithm of Eq. (5.35) to obtain

$$\ln\{\tilde{g}_N(s)\} = N\ln\left[1-\left\{\Gamma(1-\beta)\frac{s^\beta}{N}-\frac{1}{N^\alpha}\sum_{n=0}^{\infty}\frac{(-1)^n s^{n+1}}{n!(n+1-\beta)N^{n\alpha}}\right\}\exp(s/N^\alpha)\right] \tag{5.48}$$

Expanding Eq. (5.48) out in inverse powers of N we obtain

$$\ln\{\tilde{g}_N(s)\} = -\Gamma(1-\beta)s^\beta + \frac{1}{(1-\beta)}\frac{s}{N^{\alpha-1}} - \tfrac{1}{2}\Gamma^2(1-\beta)\frac{s^{2\beta}}{N} + O\left[N^{-2}, N^{-\alpha}\right] \tag{5.49}$$

Re-exponentiating and expanding out the right-hand side of the resulting equation in inverse powers of N yields

$$\tilde{g}_N(s) = \exp\{-\Gamma(1-\beta)s^\beta\}\left\{1+(1-\beta)^{-1}\frac{s}{N^{\alpha-1}} - \tfrac{1}{2}\Gamma^2(1-\beta)\frac{s^{2\beta}}{N} + \tfrac{1}{2}(1-\beta)^{-2}\frac{s^2}{N^{2\alpha-2}} + O\left[N^{-2}, N^{-\alpha}, N^{-(3\alpha-3)}\right]\right\} \tag{5.50}$$

The order of dominance of the terms on the right-hand side of Eq. (5.50) depends on the value of $\alpha = 1/\beta$. For $\beta < ½$ the $1/N$ term dominates, while for $½ < \beta < 1$ the $1/N^{\alpha-1}$ term is dominant. Inversion of Eq. (5.50) can be performed term-by-term. We have, for example

$$L^{-1}[s\exp(-\gamma s^\beta)] = \frac{d}{dt}g_\infty(t,\gamma) + g_\infty(0,\gamma) = \frac{d}{dt}g_\infty(t,\gamma) \tag{5.51}$$

$$L^{-1}[s^2\exp(-\gamma s^\beta)] = \frac{d}{dt}\left\{\frac{d}{dt}g_\infty(t,\gamma)\right\} + \frac{d}{dt}\Big|_{t=0} g_\infty(t,\gamma) = \frac{d^2}{dt^2}g_\infty(t,\gamma) \tag{5.52}$$

and $$L^{-1}[s^{2\beta}\exp(-\gamma s^\beta)] = \frac{d^2}{d\gamma^2}g_\infty(t,\gamma) \tag{5.53}$$

We note, in writing Eqs. (5.51) and (5.52), that the value of the stable density $g_\infty(t, \gamma)$ as well as all its derivatives ia zero at $t = 0$. Eq. (2.23) may be used to relate derivatives of $g_\infty(t, \gamma)$ with respect to γ to derivatives with respect to t. We have

$$\frac{d}{d\gamma} g_\infty(t,\gamma) = -\alpha\gamma^{-\alpha-1}\left\{g_\infty(t/\gamma^\alpha;1) + t\gamma^{-\alpha} g_\infty{}'(t/\gamma^\alpha;1)\right\}$$

$$= -\alpha\gamma^{-1}\left\{g_\infty(t;\gamma) + t g_\infty{}'(t;\gamma)\right\} = -\alpha\gamma^{-1}\frac{d}{dt}\{t g_\infty(t;\gamma)\} \tag{5.54}$$

and $$\frac{d^2}{d\gamma^2} g_\infty(t,\gamma) = \alpha\gamma^{-2}\frac{d}{dt}\{t g_\infty(t;\gamma)\} + \alpha^2\gamma^{-2}\frac{d}{dt}\left\{t\frac{d}{dt}\{t g_\infty(t;\gamma)\}\right\}$$

$$\frac{d^2}{d\gamma^2} g_\infty(t,\gamma) = \alpha\gamma^{-2}\frac{d}{dt}\left\{\{t g_\infty(t;\gamma)\} + \alpha t\frac{d}{dt}\{t g_\infty(t;\gamma)\}\right\} \tag{5.55}$$

Using Eqs. (5.51)-(5.53), together with Eq. (5.55), Eq. (5.50) may be inverted to obtain

$$g_N(t) = g_\infty(t;\gamma) + \frac{1}{N^{\alpha-1}}(1-\beta)^{-1} g_\infty{}'(t;\gamma) - \tfrac{1}{2}\beta^{-2}\frac{1}{N}\frac{d}{dt}\left\{\beta t g_\infty(t;\gamma) + t\frac{d}{dt}\{t g_\infty(t;\gamma)\}\right\}$$
$$+ \tfrac{1}{2}(1-\beta)^{-2}\frac{1}{N^{2\alpha-2}} g_\infty{}''(t;\gamma) + O[N^{-2}.N^{-\alpha}, N^{-(3\alpha-3)}] \tag{5.56}$$

with $$\gamma = \Gamma(1-\beta) \tag{5.57}$$

Note that the notations $g_\infty{}'(t;\gamma)$ and $g_\infty{}''(t;\gamma)$ are shorthands for the first and second derivatives of $g_\infty(t;\gamma)$ with respect to time, respectively. Integrating Eq. (5.56) to obtain the cumulative distribution function yields

$$G_N(t) = G_\infty(t;\gamma) + \frac{1}{N^{\alpha-1}}(1-\beta)^{-1} g_\infty(t;\gamma) - \tfrac{1}{2}\beta^{-2}\frac{1}{N}\left\{\beta t g_\infty(t;\gamma) + t\frac{d}{dt}\{t g_\infty(t;\gamma)\}\right\}$$
$$+ \tfrac{1}{2}(1-\beta)^{-2}\frac{1}{N^{2\alpha-2}} g_\infty{}'(t;\gamma) + O[N^{-2}.N^{-\alpha}, N^{-(3\alpha-3)}] \tag{5.58}$$

For the special case $\beta = 2/3$, the third and fourth terms on the right-hand side of Eq. (5.58) are of the same order, and we may write

$$G_N(t) = G_\infty(t;\gamma) + a_1(t)/N^{1/2} + a_2(t)/N + O[N^{-3/2}] \tag{5.59}$$

with $$a_1(t) = 3 g_\infty(t;\gamma) \tag{5.60}$$

and $$a_2(t) = \tfrac{9}{2}\left\{g_\infty{}'(t;\gamma) - \tfrac{1}{4}t\{\tfrac{5}{3} g_\infty(t;\gamma) + t g_\infty{}'(t;\gamma)\}\right\} \tag{5.61}$$

Defining

$$h_N(t) \equiv \{G_N(t) - G_\infty(t;\gamma)\} N^{1/2} \tag{5.62}$$

we have

$$h_N(t) = a_1(t) + a_2(t) N^{-1/2} + O[N^{-1}] \tag{5.63}$$

For fixed t, $h_N(t)$ should be a linear function of $N^{-1/2}$ for N sufficiently large. Figure 5.8 shows a plot of $h_N(t)$ versus $N^{-1/2}$ for several values of t, computed using the Stehfest algorithm with 14 nodes (this was also used to compute the stable distribution as well as $G_N(t)$) . The range of N used is 100 to 1000. Though the error in the Stehfest algorithm is magnified for $h_N(t)$, particularly for $G_N(t)$ close to $G_\infty(t;\gamma)$, values of $a_1(t)$ computed using Figure 5.8 are in good agreement with the theoretical expression given in Eq. (5.58). A comparison is shown in Table 5.III. The results are with about 3% of each other.

The expansion in Eq. (5.59) provides a way of addressing the dependence of the parameter on N for a fixed quartile q. Let this parameter be denoted by t_N. We then have

$$q = G_\infty(t_\infty;\gamma) = G_N(t_N) \tag{5.64}$$

Let us write

$$t_N = t_\infty + b_1(t_\infty)/N^{1/2} + b_2(t_\infty)/N + O[N^{-3/2}] \tag{5.65}$$

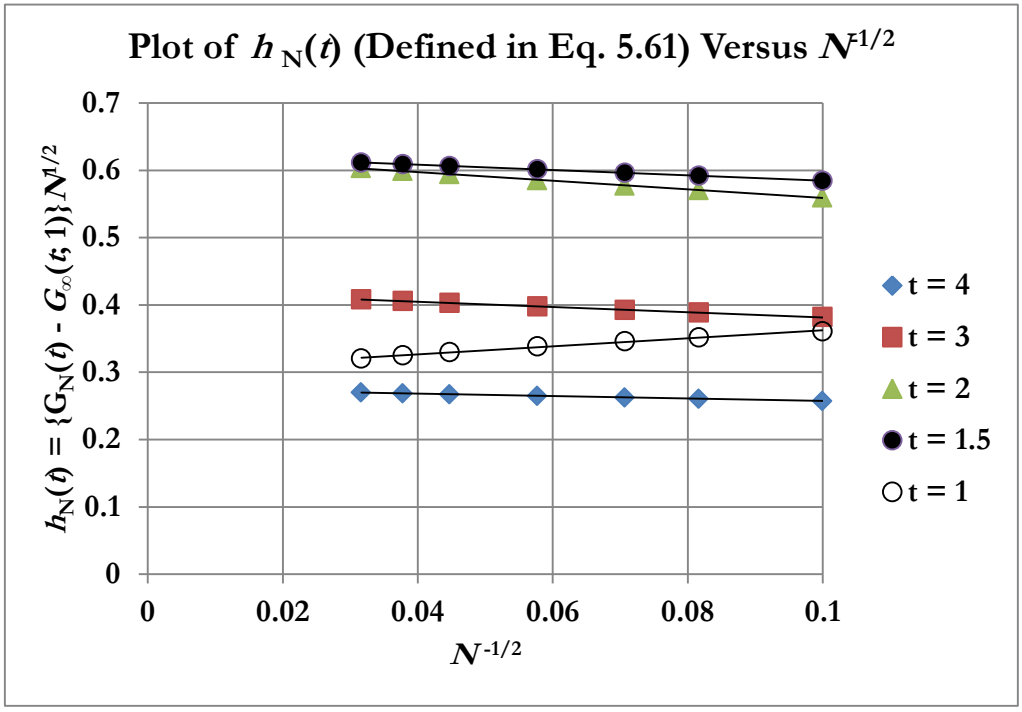

Figure 5.8. Plot of $h_N(t)$ Versus $N^{-1/2}$ for Various Values of the Parameter t.

Table 5.V. Comparison of Values of $a_1(t)$ Computed from Figure 5.7 with the Theoretical Value in Eq. (5.58).

Parameter *t*	$a_1(t)$ from Figure 5.7	$a_1(t)$ Equation 5.58
4	0.2756	0.2775
3	0.4201	0.4204
2	0.6228	0.6234
1.5	0.6238	0.6307
1	0.303	0.2891

Substituting Eq. (5.58) into Eq. (5.62) yields the result

$$G_\infty(t_\infty;\gamma) = G_\infty(t_N;\gamma) + a_1(t_N)/N^{1/2} + a_2(t_N)/N + O[N^{-3/2}] \tag{5.66}$$

Substituting Eq. (5.63) into Eq. (5.64). expanding the functions G_N and a_1 appropriately, and equating coefficients of $N^{-1/2}$ and N^{-1}, we obtain

$$G_\infty'(t_\infty;\gamma)b_1(t_\infty) + a_1(t_\infty) = 0 \tag{5.67}$$

and $$G_\infty'(t_\infty;\gamma)b_2(t_\infty) + \tfrac{1}{2}G_\infty''b_1^{\,2}(t_\infty) + a_1'(t_\infty)b_1(t_\infty) + a_2(t_\infty) = 0 \tag{5.68}$$

Noting that

$$G_\infty'(t_\infty;\gamma) = g_\infty(t_\infty;\gamma) \tag{5.69}$$

we deduce that

$$b_1(t_\infty) = -3 \tag{5.70}$$

and $$b_2(t_\infty) = -\left\{\frac{a_2(t_\infty) - \frac{9}{2}g_\infty'(t_\infty;\gamma)}{g_\infty(t_\infty;\gamma)}\right\}$$

$$= -\tfrac{9}{8}\frac{\{\frac{5}{3}g_\infty(t_\infty;\gamma) + t_\infty g_\infty'(t_\infty;\gamma) - 8g_\infty'(t_\infty;\gamma)\}}{g_\infty(t_\infty;\gamma)} \tag{5.71}$$

In Figure 5.1, the error of approximating x_N, where

$$x_N = t_N + 1/N^{1/2} \tag{5.72}$$

by $x_\infty = t_\infty$ was computed using the Stehfest algorithm and plotted in order to compare with the results of Monte-Carlo simulations reported in [2].. A better approximation for N large, suggested by Eq. (5.71), is $x_\infty - 2/N^{1/2}$. This is shown in Figure 5.9. For the 50% and 98% quartiles the new approximation is a clear improvement on the old one for all values of N (see Figure 5.9b & c). For the 2% quartile, the new approximation starts to improve on the old for N =20 or larger, with the degree of improvement increasing rapidly as N increases (see Figure 5.9a).

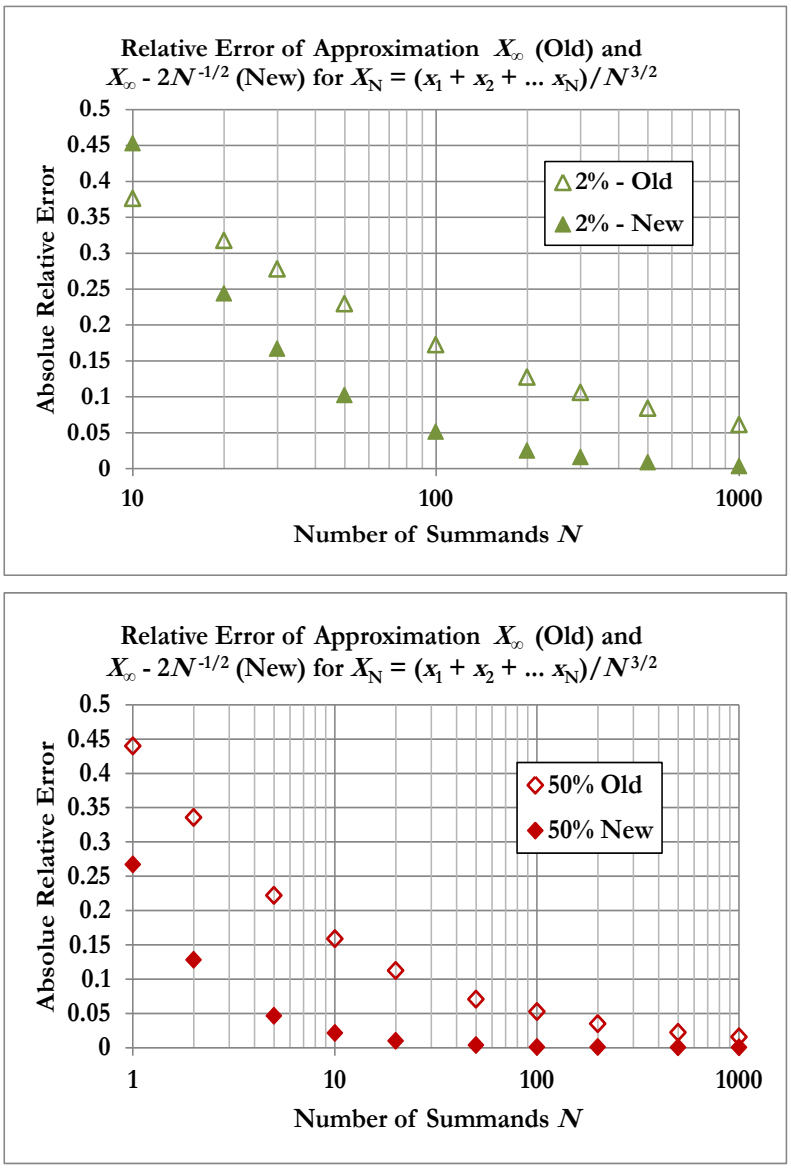

Figure 5.9 Approximation Error of $X_\infty - 2/N^{1/2}$ versus X_∞ as an Estimator for X_N. (a) 2% Quartile, (b) 50% Quartile

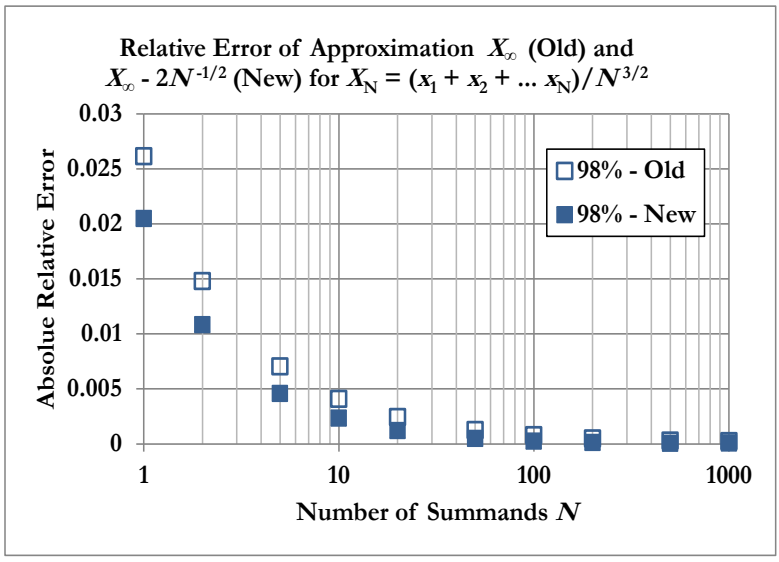

Figure 5.9 (Continued) Approximation Error of $X_\infty - 2/N^{1/2}$ versus X_∞ as an Estimator for X_N. (c) 98% Quartile.

6. Conclusions and Recommendations

In this report a novel method for evaluating quantiles of sums of Pareto-distributed variables was investigated. For sufficiently small values of the exponent β characterizing these distributions, namely $\beta \leq 2$, these distributions have "heavy" tails for large values of the parameter that yield variances that are infinite. This presents challenges for the determination of the distribution of sums of such variables, since the large body of statistical literature based on the central limit theorem is not applicable.

The application area that motivated this work is the distribution of seismic moment, which is a Pareto distribution with a β-value of around 2/3, corresponding to a *b*-value of unity in the Gutenberg-Richter law for moment magnitude. The determination of statistical properties of total moment, corresponding to the sum of the moments of individual seismic events, is important for the development of seismological models such as the strain partitioning model [1]. These properties have traditionally been obtained using intensive Monte-Carlo simulations.

The novel method described in this report is applicable to Pareto distributions with exponent β in the range $0 < \beta < 1$ (which have infinite mean as well as variance), and involves applying the Laplace transform to the density of a normalized sum of shifted variables (which is simply the product of the Laplace transforms of the densities of the individual variables, with a suitable scaling of the Laplace variable), and then inverting it numerically using the Gavers-Stefest algorithm. After validating the method using a number of test cases, it was applied to address the distribution of total seismic moment, and the quantiles computed for various numbers of seismic events were compared with those obtained in the literature using Monte-Carlo simulation. Excellent agreement was obtained.

The main advantage of the new method is that it is fast and easily implementable, either in a spreadsheet or in a simple program. These features, together with its accuracy, mean that it can be used to map out correlations relating values of total seismic moments for a given number of events to corresponding quantiles. These in turn can be used to perform maximum likelihood estimates in statistical seismology. The method should also be applicable to other natural process governed by Pareto distributions.

References

[1] Bourne, S.J., Oates, S., van Elk, J. & Doornhof, D. (2014), A Seismological Model for Earthquakes Induced by Fluid Extraction from a Subsurface Reservoir. *Journal of Geophysical Research: Solid Earth* in press (accepted 14th November 2014).

[2] Zaliapin, I.V., Kagan, Y.Y. & Schoenberg, F.P. (2005), Approximating the Distribution of Pareto Sums. *Pure & Applied Geophysics* 162, 1187-1228

[3] McCulloch, J.H. & Panton, D.B. (1997), Precise Tabulation of the Maximally-skewed Stable Distributions and Densities, *Comput. Statist. Data Anal.* 23, 307–320; See also Erratum, *Ibid.* 26, 101. The tabulation is available online at http://www.econ.ohio-state.edu/jhm/fracden

[4] Zolotarev, V.M. (1954), Expression of the Density of a Stable Distribution with Exponent α Greater than One by Means of a Density with Exponent $1/\alpha$, (in Russian), *Dokl. Akad. Nauk SSSR* 98, 735–738.

[5] Abramowitz, M. & Stegun, A., G., (Eds.), (1972), Handbook of Mathematical Functions, with Formulas, Graphs and Tables. *National Bureau of Standards Applied Mathematics Series 55*. Chapter 13, Sections 13.1 & 13.2, Pages 504-505.

[6] See Reference [4], Eq. 13.1.33 on Page 504 and Eq. 13.2.5 on Page 505.

[7] Abramowitz, M. & Stegun, A., G., (Eds.), (1972), Handbook of Mathematical Functions, with Formulas, Graphs and Tables. *National Bureau of Standatds Applied Mathematics Series 55*. Chapter 6, Section 6.2, Eqs. 6.2.1 & 6.2.2 , Page 258.

[8] Abramowitz, M. & Stegun, A., G., (Eds.), (1972), Handbook of Mathematical Functions, with Formulas, Graphs and Tables. *National Bureau of Standatds Applied Mathematics Series 55*. Chapter 6, Section 6.1, Eq. 6.1.17, Page 256.

[9] Gaver, D.P. Jr,. 1966, Observing Stochastic Processes, and Approximate Transform Inversion. *Operations Research* 14 (3), 444-459.

[10] Stehfest, H., 1970, Algorithm: Numerical Inversion of Laplace Transforms. *Communications of the ACM* 13 (1), 47-49.

[11] Abate, J. & Whitt, W., 2006, A Unified Framework for Numerically Inverting Laplace Transforms. *INFORMS J. Computation* 18, 408-421.

[12] Harris, C., van Dorp, J. & Giuliani, V. (2014), Near-Electrode Effects in Formation Joule Heating. *Internal Shell report SR.13.13269*, issued February 2014.

[13] Alain Gringarten, (2014), Personal Communication, Imperial College London, September 2014.

[14] Goldstein, S., (1932), Some Two-Dimensional Diffusion Problems with Circular Symmetry. *Proc. London Math. Soc.* 34-2 (1) 51-88.

[15] Ritchie, R.H. & Sakakura, A.Y., 1956, Asymptotic Expansions of Solutions of the Heat Conduction Equation in Internally Bounded Cylindrical Geometry. *J. Applied Phys.* 37 (12), 1453-1459.

[16] Carslaw, H.G and Jeager, H.C., 1959, Conduction of Heat in Solids, Second Edition. *Oxford Science Publications, Oxford University Press.* ISBN 978-0-19-853368-9, pp 339-341.

[17] http://keisan.casio.com/exec/system/1349144276

Appendix A – Expression of Eq, (4.18) in Terms of Error Functions

The integral appearing on the right-hand side of Eq. (4.18) takes the form

$$I_n(\alpha,\beta)=\int_0^\infty du u^n \exp(-\alpha u-\beta u^2) \tag{A.1}$$

Replacing n by n -1 in Eq. (A.1) and integrating by parts, we obtain

$$I_{n-1}(\alpha,\beta)=\left[(u^n/n)\exp(-\alpha u-\beta u^2)\right]_0^\infty+\frac{1}{n}\int_0^\infty du u^n(\alpha+2\beta u)\exp(-\alpha u-\beta u^2) \tag{A.2}$$

The integrated term vanishes, and we deduce that

$$I_{n-1}(\alpha,\beta)=\frac{1}{n}\{\alpha I_n(\alpha,\beta)+2\beta I_{n+1}(\alpha,\beta)\} \tag{A.3}$$

Eq. (A.3) can be rearranged to read

$$I_{n+1}(\alpha,\beta)=\frac{1}{2\beta}\{nI_{n-1}(\alpha,\beta)-I_n(\alpha,\beta)\} \tag{A.4}$$

Thus if we have expressions for I_0 and I_1, expressions for I_n, n = 2, 3, … may be obtained successively by using Eq. (A.4). Note that we may write

$$I_0(\alpha,\beta)=\exp\{\alpha^2/(4\beta)\}\frac{2}{\sqrt{\pi}}\int_0^\infty du\exp\{-\beta(u+\alpha/(2\beta)\}^2$$

$$=\beta^{-1/2}\exp\{\alpha^2/(4\beta)\}\frac{2}{\sqrt{\pi}}\int_{\alpha/(2\sqrt{\beta})}^\infty dw\exp(-w^2)=\beta^{-1/2}\exp\{\alpha^2/(4\beta)\}\mathrm{erfc}\{\alpha/(2\sqrt{\beta})\} \tag{A.5}$$

For $I_1(\alpha, \beta)$, we write

$$I_1(\alpha,\beta)=\frac{1}{2\beta}\frac{2}{\sqrt{\pi}}\int_0^\infty du\{\alpha+2\beta u\}\exp(-\alpha u-\beta u^2)-\frac{\alpha}{2\beta}I_0(\alpha,\beta)$$

$$=\frac{1}{2\beta}\frac{2}{\sqrt{\pi}}\left[-\exp(-\alpha u-\beta u^2)\right]_0^\infty-\frac{\alpha}{2\beta}I_0(\alpha,\beta)$$

$$=\frac{1}{\sqrt{\pi}\beta}-\frac{\alpha}{2\beta}I_0(\alpha,\beta) \tag{A.6}$$

Substituting Eq. (A.5) into Eq. (A.6), we get

$$I_1(\alpha,\beta)=\frac{1}{\sqrt{\pi}\beta}-\tfrac{1}{2}\alpha\beta^{-3/2}\exp\{\alpha^2/(4\beta)\}\mathrm{erfc}\{\alpha/(2\sqrt{\beta})\} \tag{A.7}$$

Example

Eq. (4.10) may be written as

$$g(t)=\tfrac{1}{4}t^{-3/2}I_1(1,(4t)^{-1})=\frac{1}{\sqrt{\pi t}}-\exp(t)\mathrm{erfc}(\sqrt{t}) \tag{A.8}$$

Thus we recover Eq. (4.16).

Inspection of Eq. (4.18) shows that this can be written in the form

$$g_N(\tilde{t}_S) = \frac{N^N}{(N-1)!}\frac{1}{4\tilde{t}_S^{3/2}} I_N(N,(4\tilde{t}_S)^{-1}) \qquad \text{(A.8)}$$

For small values of *N*, the procedure described in this appendix may be used to compute $g_N(\tilde{t}_S)$. Round-off errors render the procedure impractical for *N* greater than about 5. The is because $I_N(N,(4\tilde{t}_S)^{-1})$ decreases exponentially as *N* increases, yet it is computed from the differences of much larger quantities.

Appendix B – Distribution of The Sum of Two Pareto Variables With $\beta = ½$

The probability density function for the sum x_S of two samples drawn from the Pareto distribution with the density given in Eq. (2.2) takes the following form

$$f(x_S) = \beta^2 \int_1^{x_S-1} dx_1 x_1^{-(1+\beta)} (x_S - x_1)^{-(1+\beta)} \; ; x_S \geq 2$$
$$= 0 \text{ , otherwise} \tag{B.1}$$

Making the change of variable

$$\xi = x_1 / x_S \tag{B.2}$$

yields the result

$$f(x_S) = \beta^2 x_S^{-(1+2\beta)} \int_{1/x_S}^{1-1/x_S} d\xi \xi^{-(1+\beta)} (1-\xi)^{-(1+\beta)} \tag{B.3}$$

The corresponding distribution is

$$F(x_S) = \beta^2 \int_2^{x_S} dx x^{-(1+2\beta)} \int_{1/x}^{1-1/x} d\xi \xi^{-(1+\beta)} (1-\xi)^{-(1+\beta)} \tag{B.4}$$

The expression on the right-hand side of Eq. (B.4) may be reduced to a single integration by integrating by parts:

$$F(x_S) = \left[-\tfrac{1}{2}\beta x^{-2\beta} \int_{1/x}^{1-1/x} d\xi \xi^{-(1+\beta)} (1-\xi)^{-(1+\beta)} \right]_2^{x_S} + \beta \int_2^{x_S} dx x^{-2\beta-2} (1-1/x)^{-(1+\beta)} x^{1+\beta}$$
$$= \beta \int_2^{x_S} dx (x-1)^{-(1+\beta)} - \tfrac{1}{2}\beta x_S^{-2\beta} \int_{1/x_S}^{1-1/x_S} d\xi \xi^{-(1+\beta)} (1-\xi)^{-(1+\beta)}$$
$$= 1 - (x_S - 1)^{-\beta} - \tfrac{1}{2}\beta x_S^{-2\beta} \int_{1/x_S}^{1-1/x_S} d\xi \xi^{-(1+\beta)} (1-\xi)^{-(1+\beta)} \tag{B.5}$$

The second integral is an incomplete Beta function and may be further transformed by setting

$$\eta = \tfrac{1}{2} - \xi \tag{B.6}$$

Then $$\int_{1/x_S}^{1-1/x_S} d\xi \xi^{-(1+\beta)} (1-\xi)^{-(1+\beta)} = \int_{1/x_S-1/2}^{1/2-1/x_S} d\eta (\tfrac{1}{4} - \eta^2)^{-(1+\beta)} = 2 \int_0^{1/2-1/x_S} d\eta (\tfrac{1}{4} - \eta^2)^{-(1+\beta)} \tag{B.7}$$

Hence,

$$1 - (x_S - 1)^{-\beta} - \beta x_S^{-2\beta} \int_0^{1/2-1/x_S} d\eta (\tfrac{1}{4} - \eta^2)^{-(1+\beta)} \tag{B.8}$$

Setting $\beta = 1/2$, we note that

$$\int_0^{1/2-1/x_S} d\eta\left(\tfrac{1}{4}-\eta^2\right)^{-3/2} = \left[\frac{4\eta}{\sqrt{\tfrac{1}{4}-\eta^2}}\right]_0^{1/2-1/x_S} = \frac{2(x_S-2)}{\sqrt{x_S-1}} \tag{B.9}$$

Then $F(x_S) = 1 - \frac{1}{\sqrt{x_S-1}}\left\{1+\frac{(x_S-2)}{x_S}\right\} = 1 - 2\sqrt{x_S-1}/x_S$ (B.10)

which establishes the result in Eq. (5.9).

Bibliographic information

Classification	Restricted
Report Number	SR.15.10646
Title	Computing the Distribution of Pareto Sums using Laplace Transformation and Stehfest Inversion
Author(s)	Christopher K Harris & Stephen J. Bourne (GSNL-PTI/RC)
Keywords	Statistical Seismicity, Pareto Sum, Total Seismic Moment, Long-Tailed Distributions, Stehfest Inversion
Date of Issue	April 2015
Period of Work	June-December 2014
US Export Control	Non US – No disclosure of Technology
WBSE Code	ZZPT/015656/010125
Reviewed by	Phil Jonathan GSUK-PTD/TASE
Approved by	Stephen Bourne (GSNL-PTI/R)
Sponsoring Company / Customer	Nederlandse Aardolie Maatschappij (NAM)
Issuing Company	Shell International Exploration and Production P.O. Box 60 2280 AB Rijswijk The Netherlands

Report distribution

Electronic distribution (PDF)

Name, Company, Ref. Ind.	*PDF*
PT Information Services, PTT/TIKE, PT-Information-Services@Shell.com	MS Word + PDF
Harris, Christopher GSNL-PTI/RC	PDF
Bourne, Stephen GSNL-PTI/RC	PDF
Jonathan, Philip GSUK-PTD/TASE	PDF
Van Elk, Jan NAM-UIO/T/DL	PDF
Van Dorp, Johan NAM-UIO/T/DL	PDF
Mossop, Tony GSNL-PTI/RC	PDF
Wentinck, Rick M GSNL-PTI/RC	PDF
Oates, Steve GSNL-PTU/E/S	PDF
Schutjens, Peter GSNL-PTU/E/Q	PDF
Bierman, Stijn GSNL-PTD/TASE	PDF
Park, Tim A GSUK-PTD/TASE	PDF